Journal homepage www.jzs.univsul.edu.iq
Journal of Zankoy Sulaimani
Part-A- (Pure and Applied Sciences)

Paleostress analysis from brittle failure and minor structures in Dokan Area, Kurdistan Region, NE of Iraq

Salim. H. Sulaiman Al-Hakari[1,]

1. Department of Geology, University of Sulaimani
E-mail : salim.sulaiman@univsul.edu.iq

Article info

Original: 14.09.2015
Revised: 17.01.2016
Accepted:30.01.2016
Published online: 20.06.2016

Key Words:
Paleostress analysis, Micro tectonic analysis, Brittle frailer analysis

Abstract

The study area is located within the high folded of the northwestern segment of the Zagros Foreland Fold Thrust Belt in northeast of Iraq. Joints, mesofaults, veins and stylolites were studied through seven stations in the Kosrat Anticline. The trend of the fold and the strike of the strata are of NW-SE direction in accordance with the main trend of Zagros folds.

New geological map and cross section of the study area were constructed. The exposed rocks of the studied area range in age from Cretaceous up to the Eocene included the following formations (Qamchuqa, Kometan, Shiranish, Tanjero, Kolosh and Sinjar) Kometan and Tanjero formations was taken in consideration for brittle failure analysis . The analyzed structural field data indicate that the investigated area was subjected throughout its geological history to four stress phases. First is primary compressive tectonic phase in the directions N-S, NE-SW and successive phase in the direction ENE-WSW. The second compressive tectonic stress in the direction NW-SE considered as a secondary phase. Third was extension tectonic phase in the direction NE-SW which developed during the final uplift stage of folding is normal to the major folds trend. The fourth is NW-SE extension face considerate as extension stress related to the primary NE-SW compressive stress.

1: Introduction:

Deformation structures that can be observed directly in individual outcrops or with the in hand specimen are commonly referred to as minor structures or mesostructures such as (Joints, striated fault planes, veins arrays, brittle shear zones and so on). They nevertheless underpin many structural interpretations. They are the building blocks that allow understanding of larger scale structures. In structural and tectonic studies these minor structures become widely known because they can be interpreted more accurately *[12]* and *[16]*

Nevertheless, the same approach and methods cannot be used for studying both small and large structures, for example small faults, and sometimes those of an intermediate size, can be observed and studied at outcrops some meters or hundreds of meters in size. Large structures on the other hand, are mainly studied using geological maps prepared from field studies and also from geophysical investigations or from interpretation of aerial photographs or satellite images *[5]*.

Pressure solution surfaces (stylolite seams) and veins arrays were carried out in the studied area for unwinding the tectonic history and detecting tectonic episodes responsible for the initiation and modification of such minor structures. Kosrat Anticline located in the high folded zone of the Zagros Fold Thrust Belt in north eastern Iraq, next to the Zagros Main Thrusts, it lies between longitudes (44° 53' 34" and 44° 58' 10") East and latitudes (35° 56' 38" and 36° 01' 46") North in the Iraqi Kurdistan Region in

Sulaimaniyah Province on the western bank of the Dokan lake (Fig. 1&2).

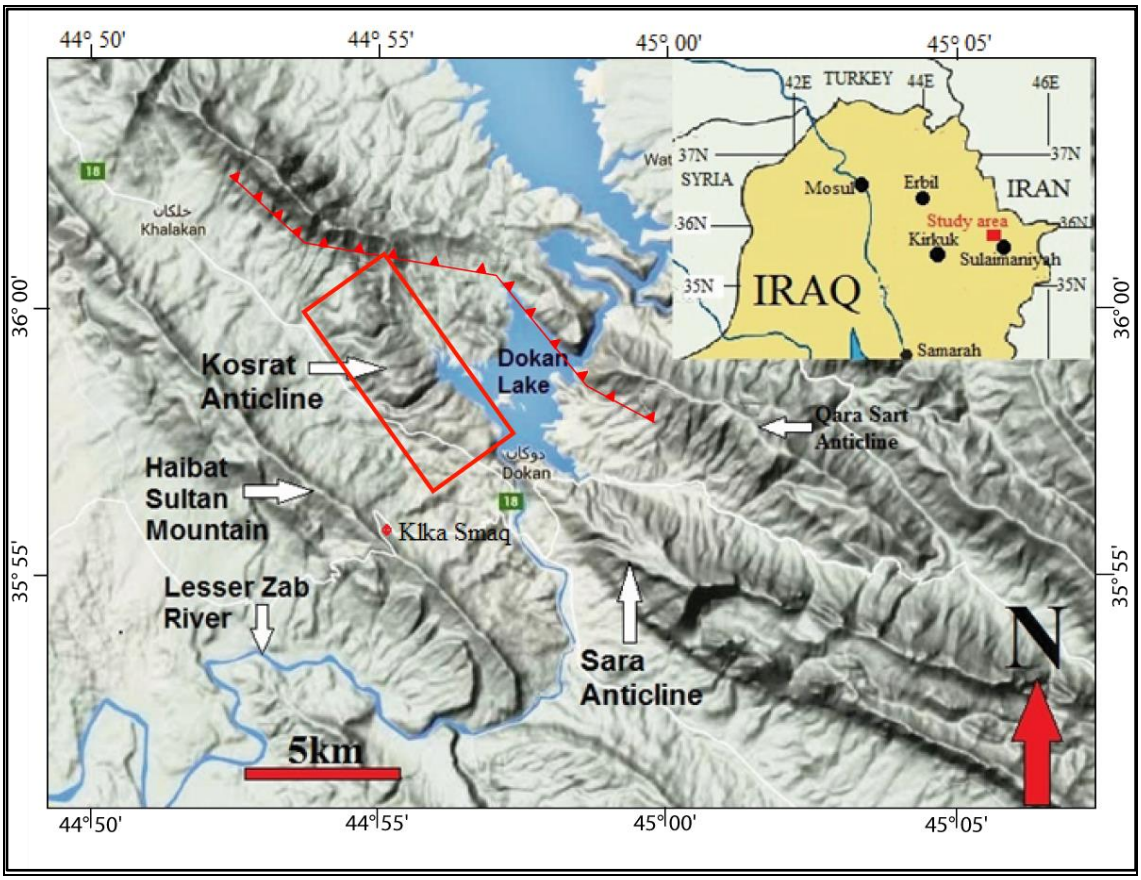

Fig.1: Location map of the study area from Google maps.

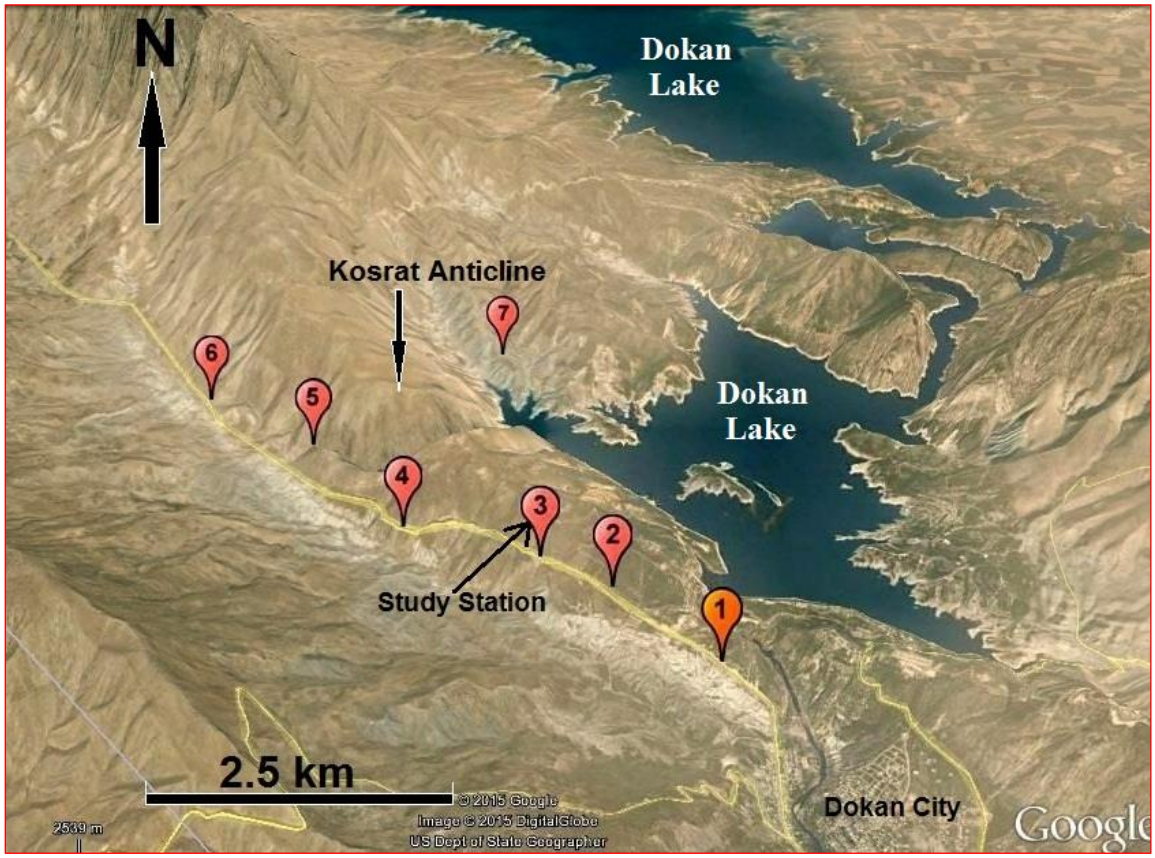

Fig.2: Location map of the study area from Google Earth shows studied stations.

1.2: Geology of the area:

As the other structures of the area, Kosrat anticline follows the general Zagros fold trend NW-SE**.**
The investigated traverse of Kosrat Anticline revealed that the anticline is asymmetrical. The southwestern limb is slightly steeper and shorter than the northeastern limb which makes this anticline vergent towards SW direction). The southeastern plunge of the anticline is near Dokan dam site and the northwestern plunge is not clear. The synoptic stereographic pi-diagram of the Kosrat anticline is shown in the (Fig.3). The vergence of the anticline is to the southwest, the attitude of the axial plane is 142°/85°, the average attitude for the northeastern limbs is 160°/22° and for the southwestern limb is 310°/30°, and the attitude of the fold axis is 147°/07°, the interlimb angle is 130° and here the fold is gentle according to Fleuty interlimb classification. According to (Fleuty, 1964) the fold is plunging inclined.

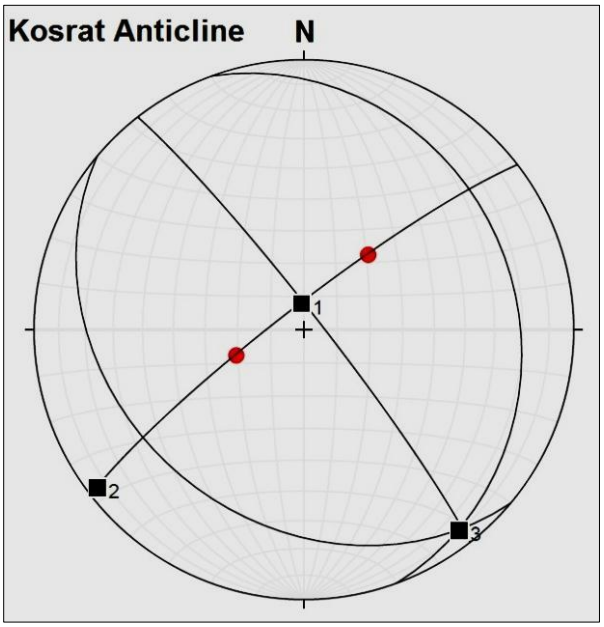

Geometry of the Kosrat anticline

The measurements are in (RHRL)

NE limb: **160°/22°**

SW limb: **310°/30°**

Fold axis: **142°/07°**

Axial plane: **142°/85°**

Interlimb angle: **130 °**

Fleuty interlimb classification: **Gentle fold**.

Fleuty 1964 classification: **Plunging**

Fig.3: Stereographic pi- diagram projection of Kosrat anticline

Many researches were studied paleostress in the Dokan area. These researches were done in the plunging area of Kosrat Anticline. The classification of the paleostress directions depended on the directions of the tectonic axes and direction of the strike of the bedding planes. These directions are rotated in the plunging area so the results were not being depended. Therefore the stations for this research selected far from plunging area to give the most realistic results. Furthermore updated program and methods were used.
Because the area lacks any detail geological map and cross section can be depended for scientific researches, therefore the present investigation attempts to draw geological map and cross section for the area (Fig.4) Geologically, Qamchuqa Fn. massive limestone and dolomitic limestone. (Hauterivian-Albian) exposed in the core of the anticline. This formation is overlain in the southwestern limb by about 5 meters of light colored grey and white limestone of Dokan Fn. (Cenomanian). Dokan Fn. overlain by about 2 meters of Gulneri shale Fn. (Turonian) which overlain by thin to moderately bedded white pelagic fine grained limestone with chert bands of Kometan Fn. (late Turonian-early Campanian). In the same limb Kometan Fn. Overlain by marl and marly limestone of Shiranish Fn.(Campanian). Between Kometan and Shiranish formations there are about one meter of thin glauconitic beds. To the south west Shiranish Fn. overlay by thin sandstone and shale beds changing upward to marl of Tanjero Fn. (Upper Campanian-Maastrichtian). The Cretaceous formations are exposed in the NE limb they are Qamchuqa, Kometan and Tanjero formations. Qamchuqa and Kometan formations form the carapace of the anticline (Fig. 4). Numbers of Tertiary formations are exposed in SW limb they are from older to younger (Kolosh, Sinjar, Gercus, Pila Spi, Fatha and Injana formations. In the northeastern limb we construct Qamchuqa and Kometan formations because of the difficulty of structure

and in the southwestern limb the map included Sinjar Formation as a last Tertiary formation (Fig.4)

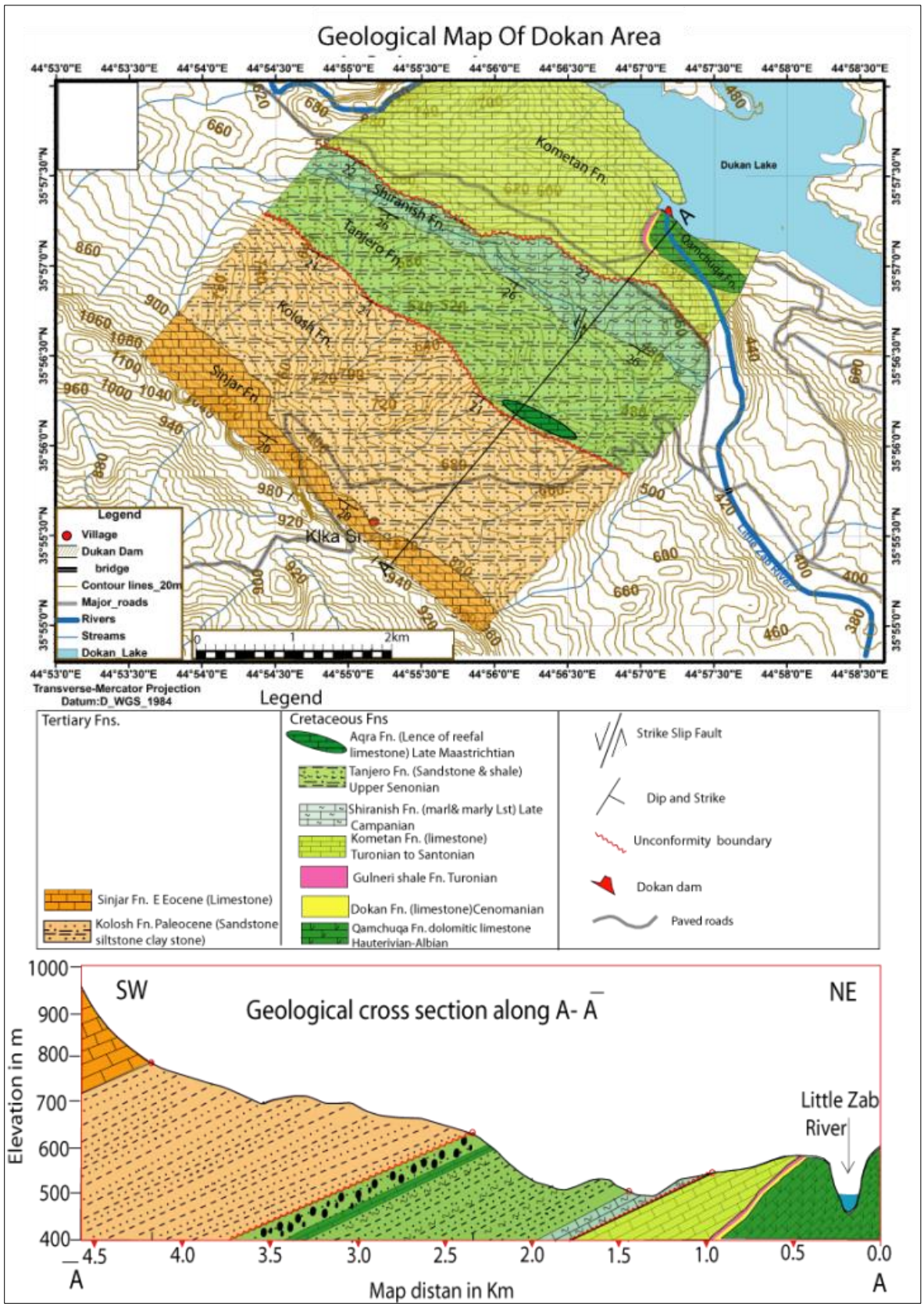

Fig.4: Geological map and cross section of Dokan area

1.4: Methodology

The field work carried out through seven stations (Fig.2). All measurement and results are in Right Hand Rule Left (RHRL). The measurements included the attitudes of bedding, joints and mesofaults (with their striations pitches and movement sense); photographs and field sketches of pressure solution seams (stylolites) and planner and enechelon vein arrays.

Joint planes data analyzed stereographically using Dips software (Dips.v5). The results of joint analysis were classified according to. *[7]*.

Win-Tensor program version 5-8-1 used for determines the paleostress directions (σ 1, σ 2, and σ 3) from the average attitudes of the conjugate joint planes. σ1 bisect acute angle between conjugate joint planes, σ3 is perpendicular to σ1 and bisect obtuse angle, and σ2 represent the line of the intersection between the two joint planes *[3]*.

Fault slips data treated by using FaultKin software (FaultKin 5.2). The software relies on Lisle's (1987). *[10]*, A-B dihedral method extension to the P & T dihedral method by Angelier and Mechler, (1977). *[4]*

Photos with the field sketches for stylolite seams, and enechelon veins were taken and interpreted. This is to deduce the orientations of maximum and minimum principal compressive stresses (σ_1, σ_3) that are responsible for the development of such brittle structures. These representations and analysis helps to describe various tectonic compressive stress episodes particularly where such structures associated with each other. Finally, the output of the kinematic analyses of various structural modes (joints, mesofaults, stylolites, and vein arrays) unified to conclude the sequence of tectonic phases which architecture the study area in the view of geotectonic setting of the studied area.

2: Paleostress Analysis:

Joints, veins, pressure solution surfaces (stylolite seams) and striated mesofaults and shear zones were analyzed for paleostress.

2.1: Joints:

Joints are among the most common of all geological features , hardly any outcrop of rock exist that does not have some types of joints through it. They provide the sequence of tectonic event during which the joints formed and the physical characteristics and impart to the rock in which they occur *[15]*.

Study of joint in rocks; however, show that the joints geometry is self-similar, which means that the joints have the same geometric pattern and spatial distribution regardless of whether the scale at which they are viewed is microscopic scale, an outcrop scale, or a regional scale *[15]*.

Because the outcrop scale is easy to observe and is the basis of most field geology, we emphasize the descriptive characteristics of joints at outcrop scale.

Joints in study area were classified according to their geometrical relations with the three perpendicular geometrical axes (**a, b &c**.). Where **(a)** is parallel to the dip direction, **(b)** is parallel to the strike direction and **(c)** is perpendicular to **a** & **b**. This classification was used by *[14]*, and followed by *([7], [8], [6], [12], [1]* (Fig.5).

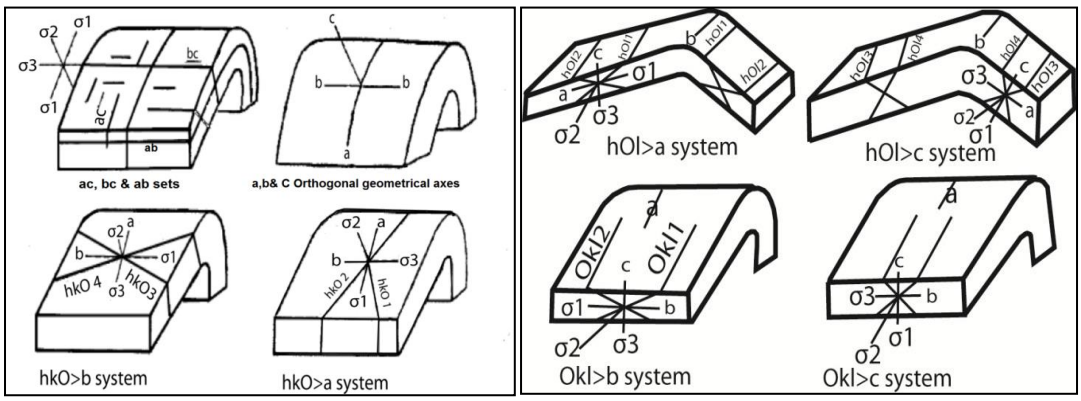

Fig. (5): Geometrical classification of the joints with respect to three orthogonal geometrical axes after (Turner and Wise, 1963 in Al-Jumaily, 2004)

2.1.1: Joint analyses in the study area:

More than (150) readings of joint planes were collected from seven stations in the study area. Strike and dip were measured for the joint planes as well as the attitude of the bedding plane which contain the joints.
The shear systems appear either as individual or conjugate systems. Many collected data were neglected due to the nonexistence of the two conjugate joints of the system in the same station.

Station one:

As shown in the figure 6 the following shear systems were recognized:
(hkO) acute about (**a**) axis , **(hkO)** acute about **(b)** axis, **(hOl)** acute about **(c)** axis and **(Okl)** acute about (**b**) axis. Paleostresses which analyzed from shear joint systems are;

Compression stress:

a) **NE-SW** compression stress from **(hkO)** acute about **(a)** axis with **(σ1)** attitudes (38°/208°) normal to sub-normal to the general trend of the major anticline. This stress state it seems as responsible to the initial folding of the anticline. (Fig. 7 left)
b) **NW-SE** compression stress from **(hkO)** acute about **(b)** with **(σ1)** attitudes (03°/308°). (Fig. 7 right)
c) **NW-SE** compression stress from **(Okl)** acute about **(b)** with **(σ1)** attitudes (07°/307°). (Fig. 8 right) b and c are in the direction parallel to sub-parallel to the trend of the major anticline.

Extension stress:

Analyzed from (**hOl)** acute about **(c)** axis with sub horizontal **(σ3)** attitude (05°/217°) associated with the final uplifting of the major fold. (Fig. 8 left). Figure 9 shows four field photos in station 1

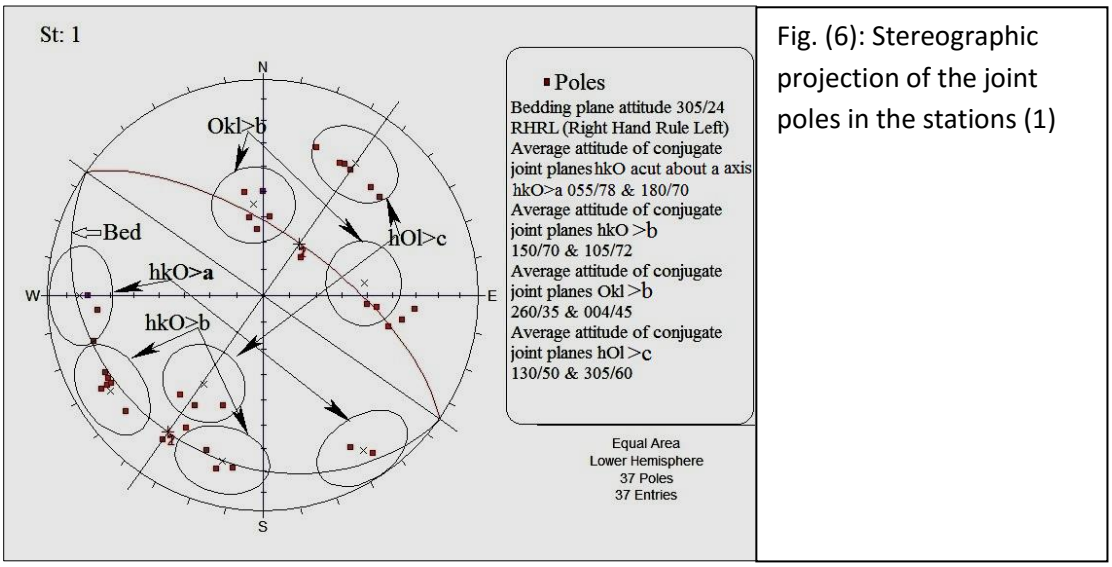

Fig. (6): Stereographic projection of the joint poles in the stations (1)

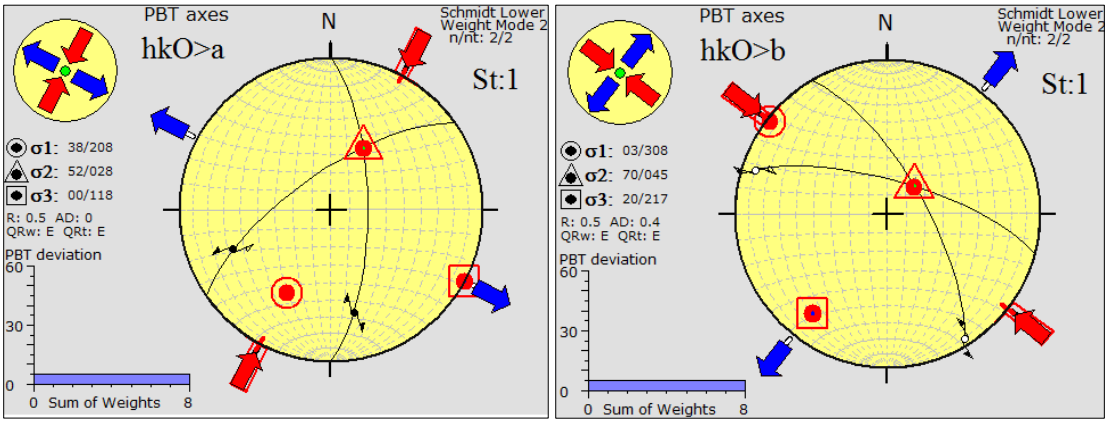

Fig. (7): Left; Paleostress analysis from hkO > a in the station 1. Right; Paleostress analysis from hkO >b in the station 1

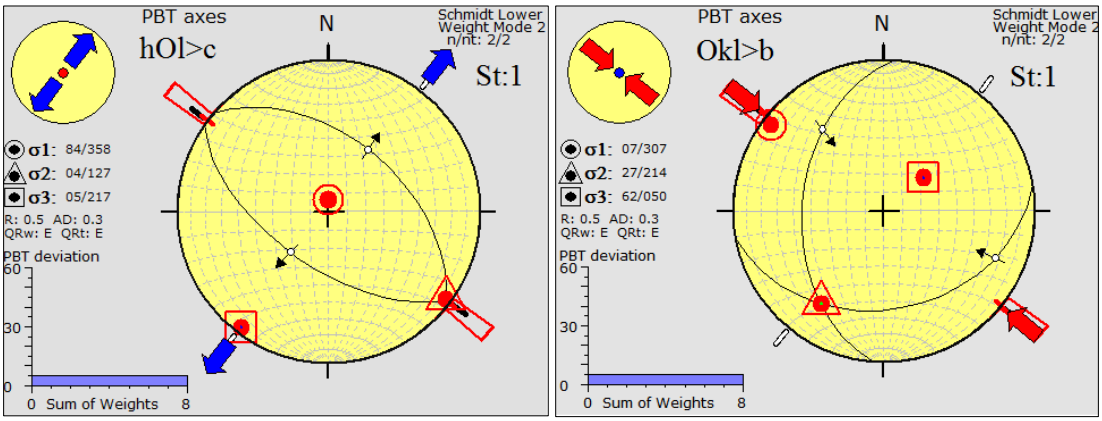

Fig. (8): Left; Paleostress analysis from hOl > c in the station 1. Right; Paleostress analysis from Okl >b in the station 1

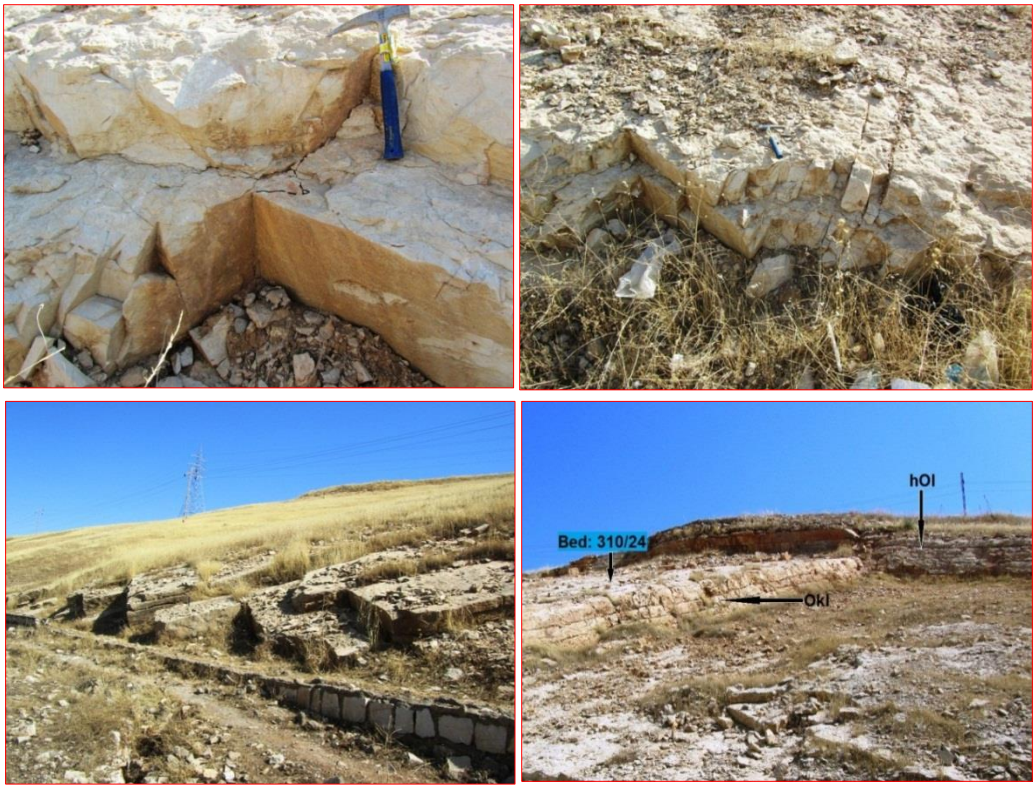

Fig. (9): Four field photos show the joints in the station 1. The photos are looking north

Fissures in station one:

There are fissures in the direction 330°. These fissures are opened along hkO acute about b joint systems which are one of the dominant joint systems in the area. These open fissures may be is one the cause of rocks fall or collapse of the rocks in the road between Dokan and Ranyah (Fig. 10). Figure (11) shows stereographic projection of the fissures.

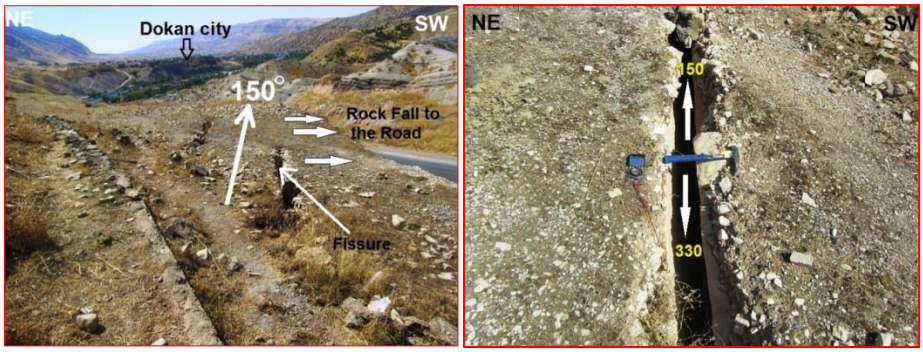

Fig. (10): Two field photos show the fissures and their direction

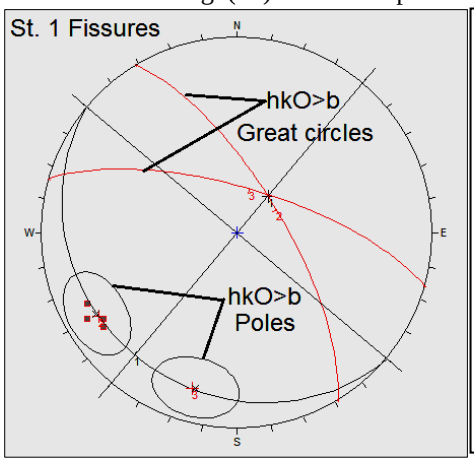

Fig. (11): Shows stereographic projection of the fissures in station one

Station two:

NE-SW compression stress from **(hkO)** acute about **(a)** axis shear systems with **(σ1)** attitude (29°/226°) was recognized in this station (Fig.12 left and right). Figure (13) shows two field photos in station 2

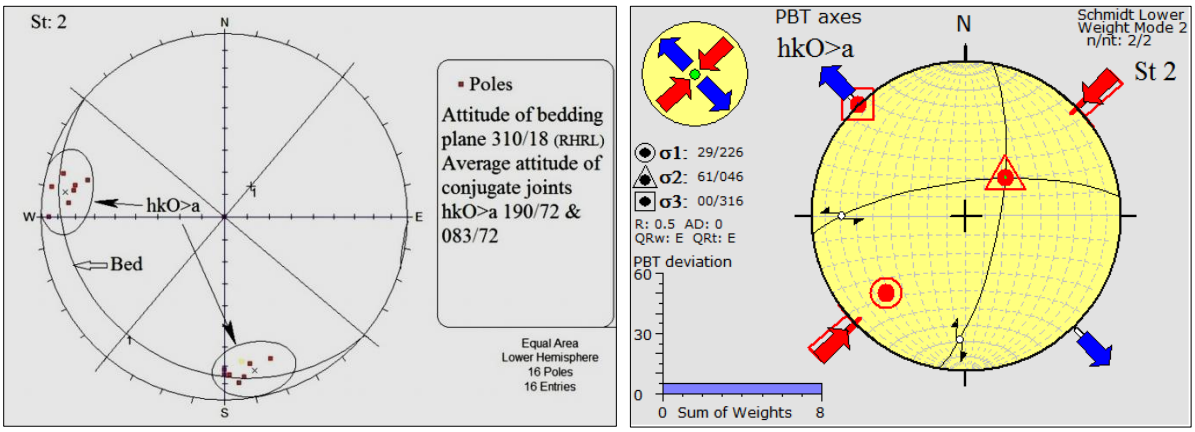

Fig. (12): left: Stereographic projection of the joint poles in the stations (2). Right: Paleostress analysis from hkO > a in the station 2

Fig. (13): Two field photos for the joints in the station 2.

Station three:

NE-SW compression stress from **(hkO)** acute about **(a)** axis shear systems with **(σ1)** attitude (13°/219°) was recognized in this station. This stress state is compatible with NE-SW stress in station 1 and 2 (Fig.14 Right). **ac** and **bc** tension sets recorded in this station with **(σ3)** attitudes(01°/131°) and

(15°/220°) respectively (Fig.15 left and Right). These two fracture directions were formed as a response to the compression stress in the direction NE-SW and NW-SE. figure 16 shows two field photos in station three.

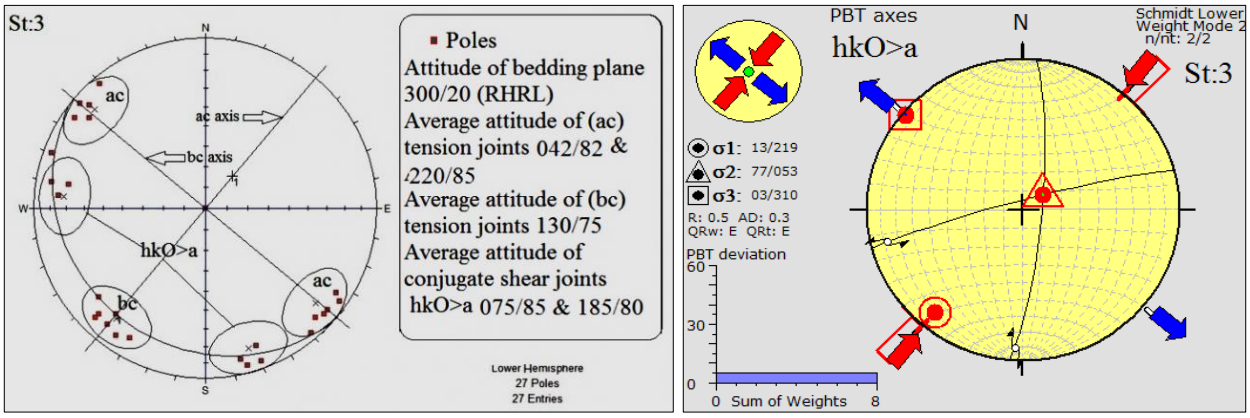

Fig. (14): left: Stereographic projection of the joint poles in the stations (3). Right: Paleostress analysis from hkO > a in the station 3.

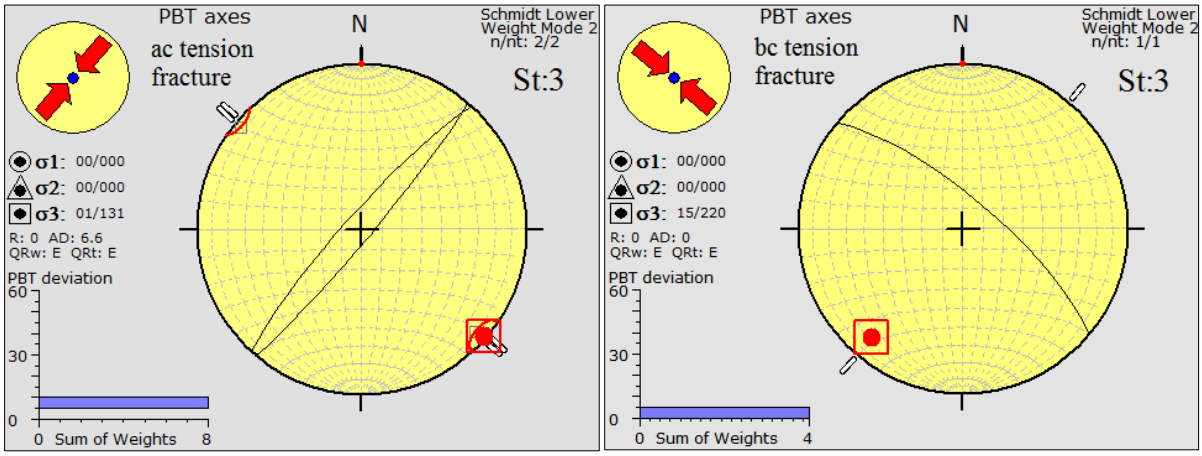

Fig. (15): left: Paleostress analysis from **(ac)** tension set joints in the station 3. Right: Paleostress analysis from **(bc)** tension set joints in the station 3.

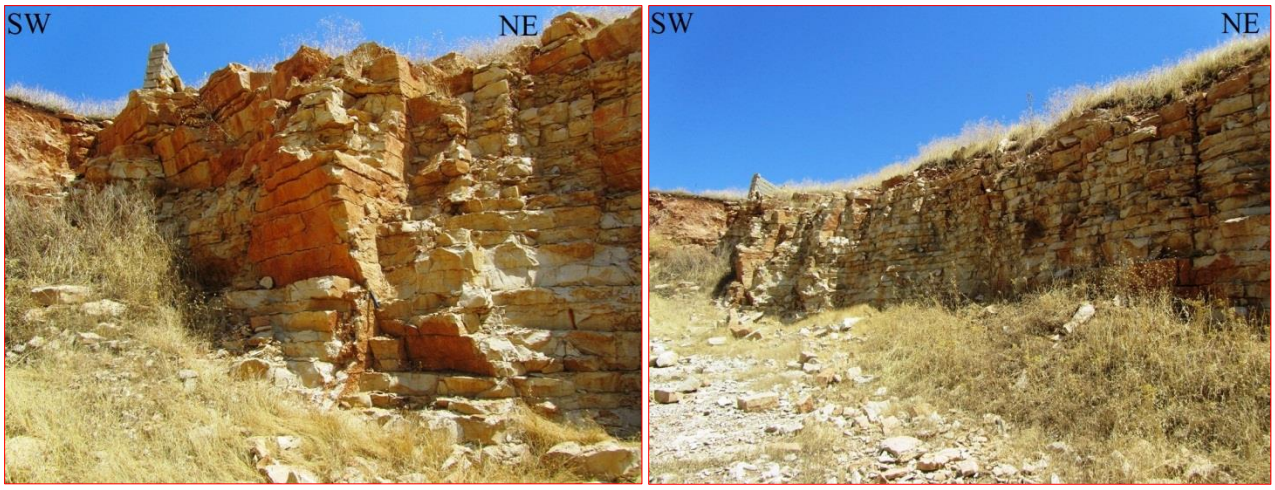

Fig. (16): Two field photos for the joints in the station 3.

Station Four:

Figure (17 Left) shows the distribution of the joints in the station four. From **(hkO)** acute about **(b)** axis shear joint system**, NW-SE** compression stress direction was analyzed with **(σ1)** attitude (04°/309°). (Fig. 17 Right)

Two extension stresses were analyzed; First from **(Okl)** acute about **(c)** axis with **(σ1)** attitude (56°/038°) and horizontal **(σ3)** attitude (01°/129°) (Fig.18 Left). Second from **(bc)** tension joints with horizontal **(σ3)** attitude (01°/228) (Fig.18 Right). Figure (19) shows two field photos in station four.

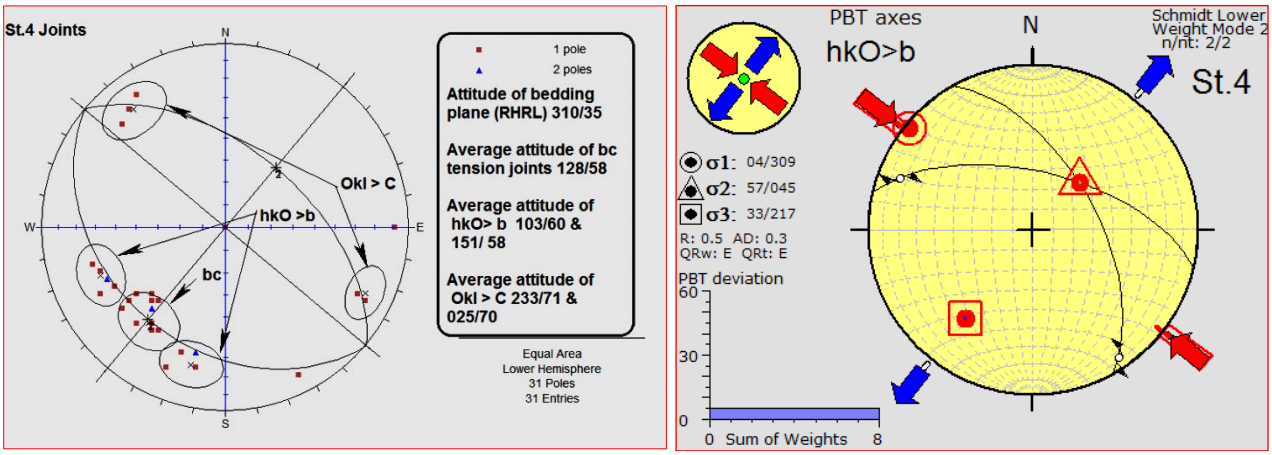

Fig. (17): left: Stereographic projection of the joint poles in the stations (4). Right: Paleostress analysis from hkO > b in the station 4.

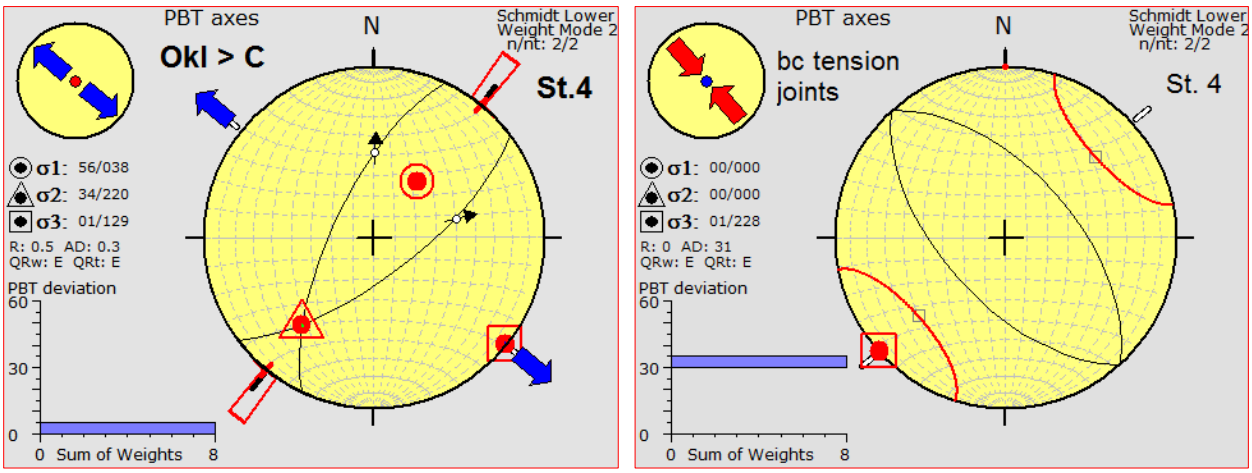

Fig. (18): left: Paleostress analysis from **(Okl> C)** joints system in the station 4. Right: Paleostress analysis from **(bc)** tension set joints in the station 4.

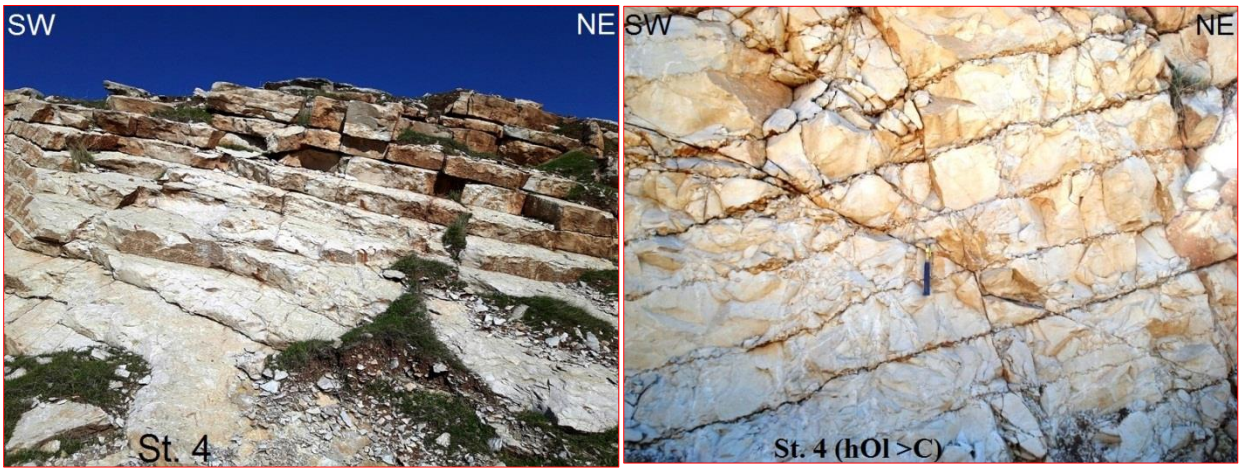

Fig. (19): Two field photos for the joints in the station 4.

Station six:

Two shear joint systems **(hkO)** acute about **(a)** with **(σ1)** attitude (21°/207°) and **(hkO)** acute about **(b)** with **(σ1)** attitude (02°/299°) were recorded in the station six (Fig. 21 left and right). Figure (20 left) shows the poles distribution of the joints. Figure (20 Right) shows field photo of the joints in station six.

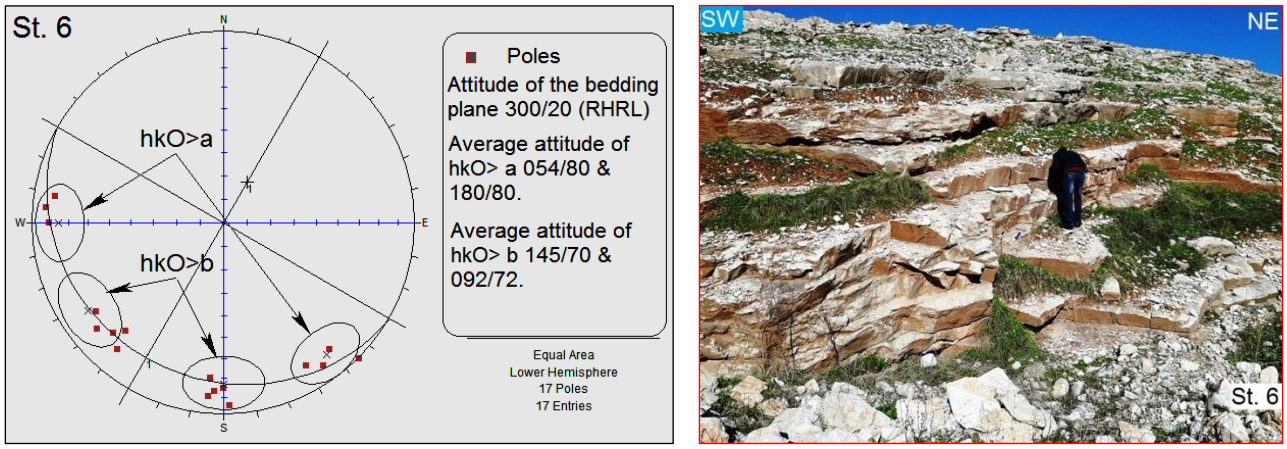

Fig. (20): left: Stereographic projection of the joint poles in the stations (6). Right: Field photo for the joints in the station (6).

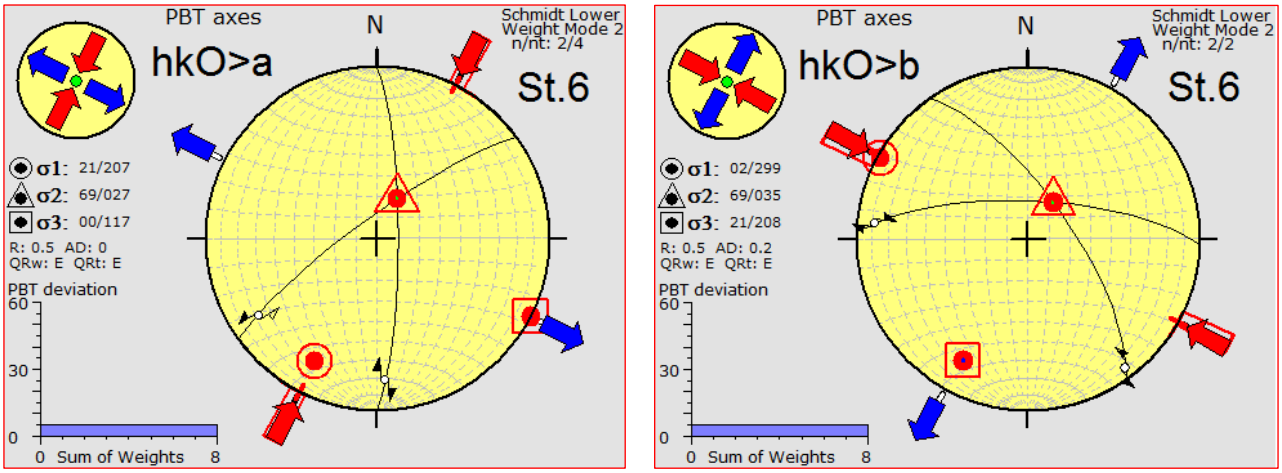

Fig. (21): Left; Paleostress analysis from hkO >a in the station 6. Right; Paleostress analysis from hkO >b in the st.6

Station seven:

This station is in the Tanjero Formation in the northeastern limb of the Kosrat anticline. More than 25 readings of joint planes were collected. Figure (22 left) shows the pole distribution of the joint planes.

Two compression stress directions were analyzed. First is **NE-SW** direction from **(hkO)** acute about **(a)** axis with **(σ1)** attitude (07°/022°) (Fig. 22 Right). Second is **NW-SE** direction from **(hkO)** acute about **(b)** axis with **(σ1)** attitude (07°/117°) fig. (23 left). Figure (23 Right) is field photos in station seven.

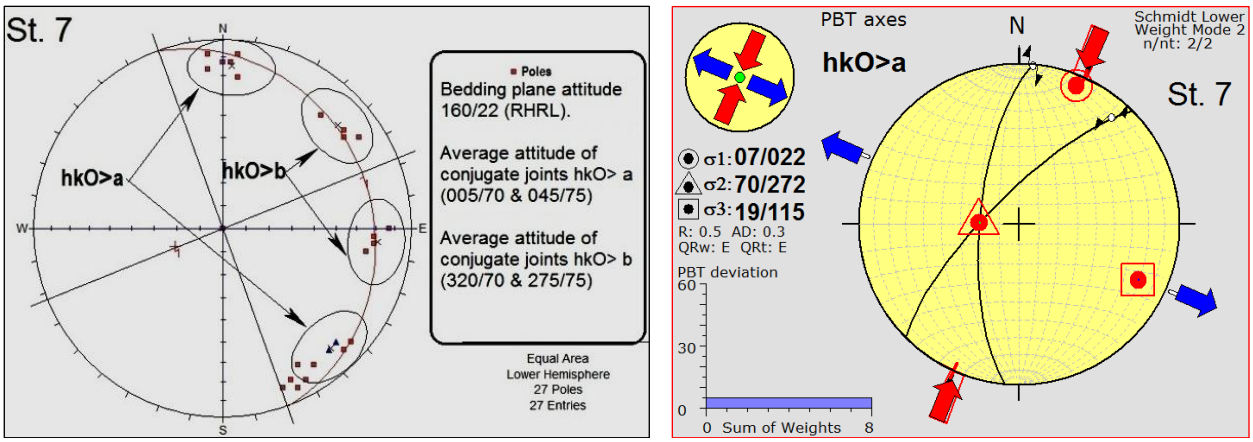

Fig. (22): left: Stereographic projection of the joint poles in the stations (7). Right: Paleostress analysis from hkO > a in the station 7.

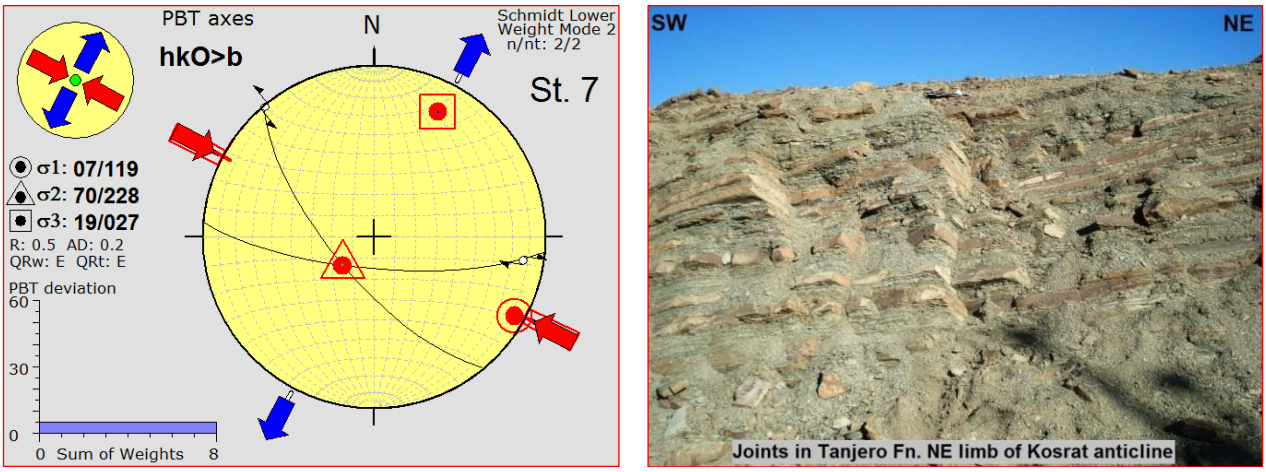

Fig. (23): left: Paleostress analysis from hkO > b in the station 7. Right: Field photo for the joints in the station (7).

Table (1) shows the paleostress directions and joints of the studied stations. From this table we can conclude that there are 15 paleostress directions measured from joint analysis distributed in the following directions: **(5** compression paleostresses in the direction NE-SW**), (5** compression Paleostresses in the direction NW-SE), **(3** extension paleostresses in the direction NE-SW**)** and **(2** extension Paleostresses in the direction NW-SE)

Table (1 Joints classification and paleostress directions in the study area

Note: all measurement results of the joints are in Right Hand Rule left (RHRL)

C: compression T: Tension

Major Fold	Fn.	Station No,	Bedding plane attitude	Type of Joints	Type of stress	Average attitude of the conjugate joint planes		Paleostress analysis			Stress direction
								σ1	σ2	σ3	
Kosrat Dokan	Kometan	1	305/24	hkO>a	C	055/78	180/70	38/208	52/028	00/118	NE-SW
				hkO>b	C	150/70	105/72	03/308	70/045	20/217	NW-SE
				Okl>b	C	260/35	004/45	07/307	27/214	62/050	NW-SE
				hOl>c	T	130/50	305/60	84/358	04/127	05/217	NE-SW
		2	310/18	hkO>a	C	190/72	083/72	29/226	61/046	00/316	NE-SW
		3	300/20	hkO>a	C	075/85	185/80	13/219	77/053	03/310	NE-SW
				ac	T	042/82	220/85	00/000	00/000	01/131	NW-SE
				bc	T	130/75		00/000	00/000	15/220	NE-SW
		4	310/35	bc	T	128/58	308/58	00/000	00/000	01/228	NE-SW
				Okl>c	T	233/71	025/70	56/038	34/220	01/129	NW-SE
				hkO>b	C	103/60	151/58	04/309	57/045	33/217	NW-SE
		6	300/20	hkO>a	C	054/80	180/80	21/207	69/027	00/117	NE-SW
				hkO>b	C	145/70	092/72	02/299	69/035	21/208	NW-SE
	Tanjero	7	160/22	hkO>a	C	005/70	045/75	07/022	70/272	19/115	NE-SW
				hkO>b	C	320/70	275/75	07/119	70/228	19/027	NW-SE

2.2: Mesofaults and paleostress analysis from fault slips data:

Different orientations of striated mesofaults assemblage were measured in the study area which has different orientations with respect to the axis of fold. The most dominated types are strike slip displacements faults. Both dextral and sinistral follow or occupy either (hkO) acute about (a) or (b) joint systems as preexisting fractures for these faults.

The measurements include of faults attitudes, pitches (Rakes) of their striations and their movement sense. This procedure can be performed by applying many software techniques written by many authors.

Station one:

Dextral and sinistral strike slip faults were recognized in this station these faults were activated on the hkO acute about b shear joints. The results of fault-slip data analysis of these faults revealed to the following states of paleostress.

Two paleostress in the directions NW-SE with **(σ1)** attitude **(20°/108°)** from dextral faults and **(14°/287°)** from sinistral faults. The two stresses are approximately in the same direction which is parallel to sub- parallel to axes of the folds (Fig.24).These stresses are compatible to same stress direction which obtained from joint analyses. Figure 25 shows the field photos of these faults.

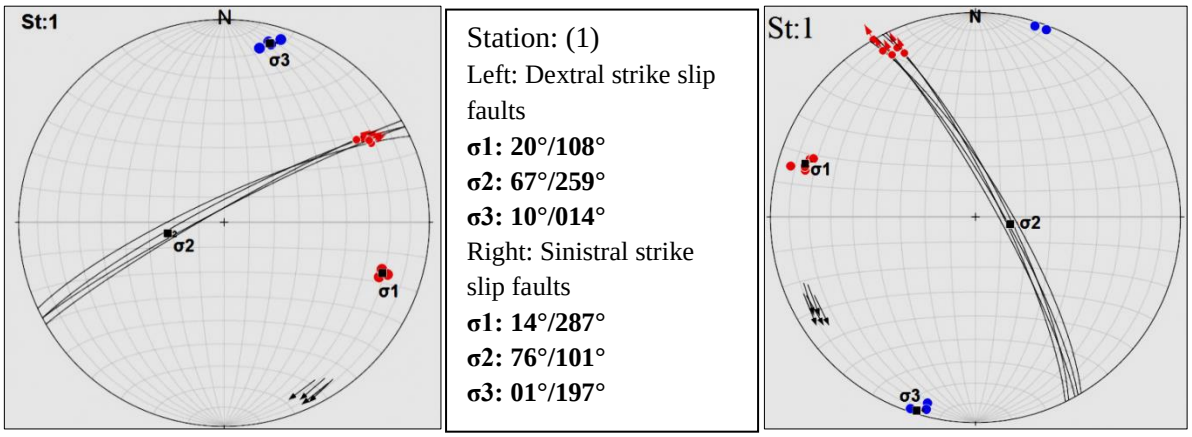

Fig. (24): Fault-slip data analyses in the station 1 from dextral and sinistral strike slip faults.

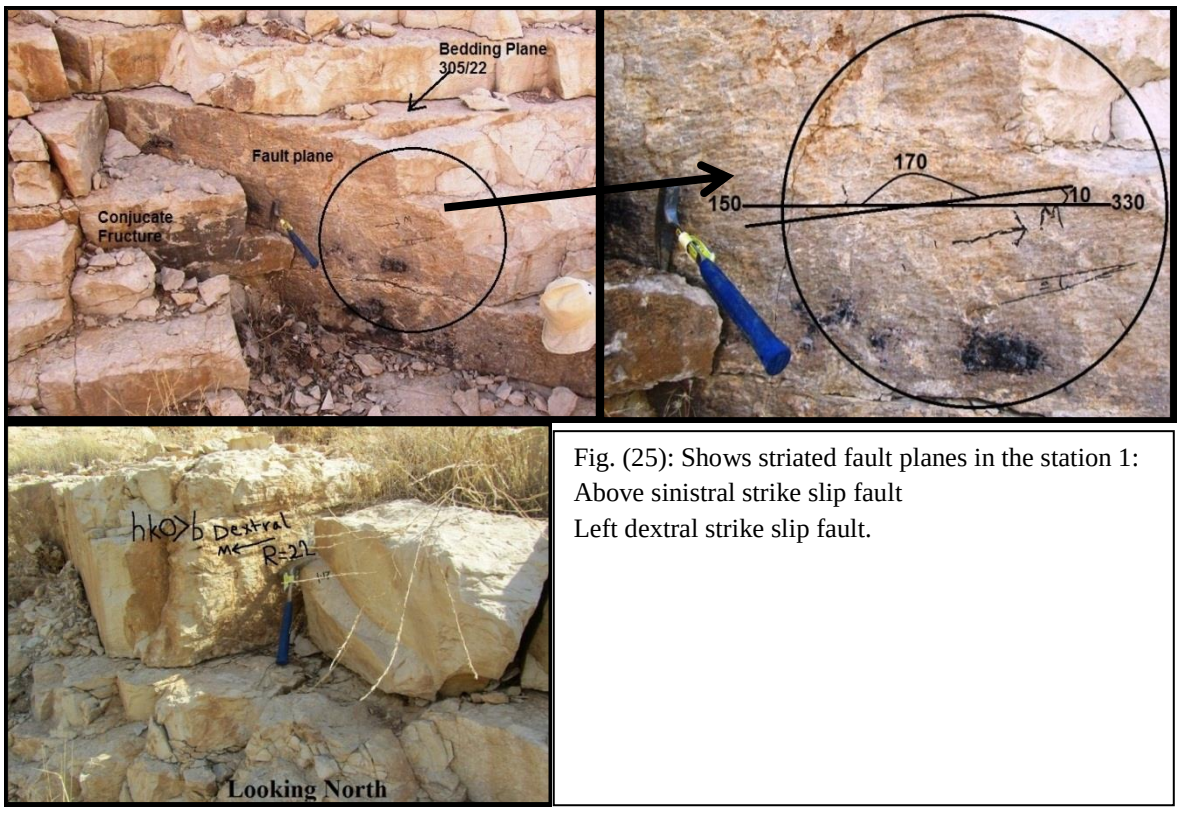

Fig. (25): Shows striated fault planes in the station 1:
Above sinistral strike slip fault
Left dextral strike slip fault.

Station two:

Three dextral strike slip faults were recorded in this station. Fault- slips data analysis of these faults revealed that the paleostress is in the direction (NE-SW) with the following principal stress directions (**σ1: 18°/217°, σ2: 70°/015° and σ3: 07°/125°)** (Fig. 26).

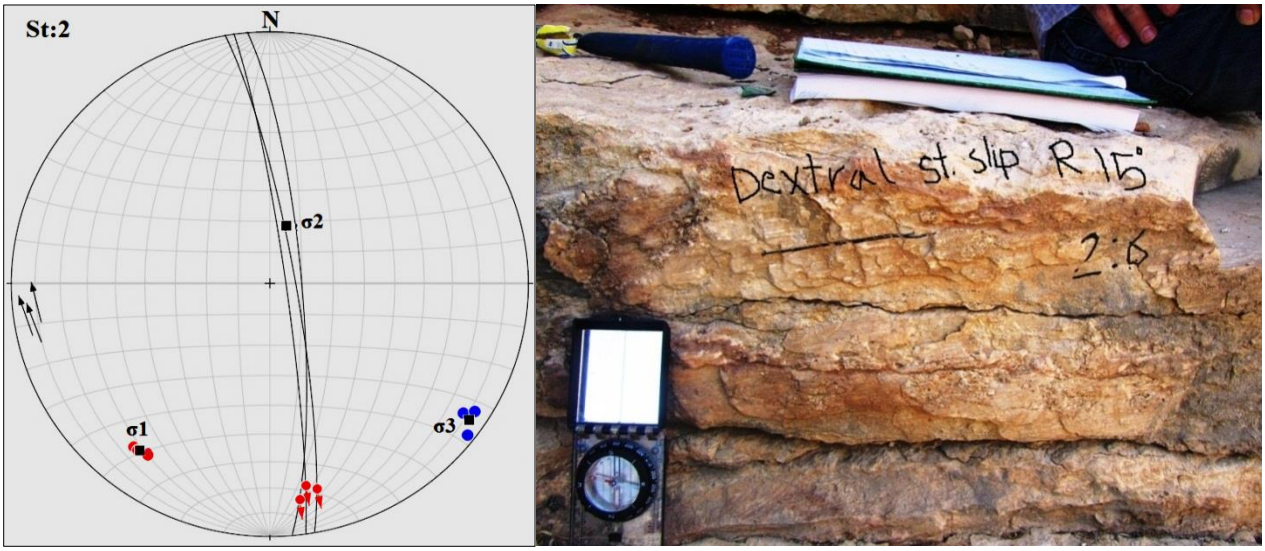

Fig. (26): Fault-slip data analyses with field photo in the station 2 from dextral strike slip faults**. (**σ1**: 18°/217°, σ2: 70°/015° and σ3: 07°/125°)**

Station three:

Two directions of sinistral strike slip faults were recorded in this station. Five faults with southeast dip direction indicate that the paleostress was approximately in the N-S direction with maximum stress axis **(σ1: 04°/178°)** (Fig.27). The second group is dipping to the NW direction. The paleostress which revealed from them indicate to the direction NE-SW with maximum stress direction **(σ1: 05°/026°)** (Fig.28). NE-SW stress direction is the main stress direction which recorded from joints and mesofaults in other stations. As we mentioned before this stress is approximately normal to the fold axes of the major folds, and they seems as responsible to the initial folding of the anticlines and different types of shear and tension fractures.

N-S compressive stress can be considered as earlier state of (NE-SW) resulted from oblique collision between the Arabian and Eurasian Plates. *[11]* and *[2]*, and also due to the counterclockwise rotation of the Arabian plate with respect to the Eurasian (Iranian) plates. [7]

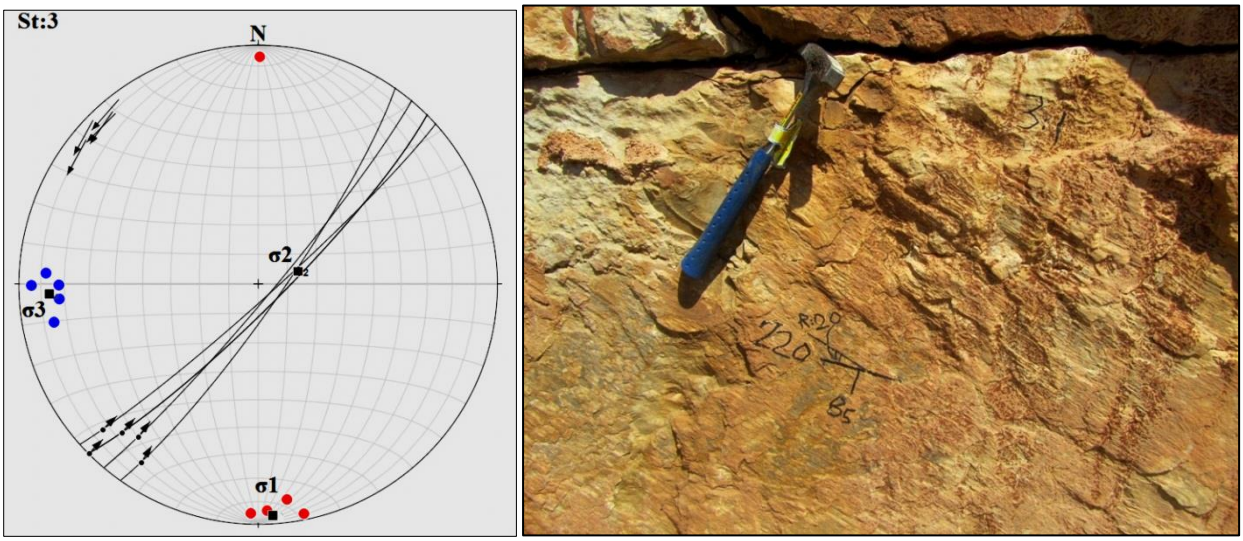

Fig. (27): Fault-slip data analyses with field photo in the station 3 from SE dipping sinistral strike slip faults**. (**σ1**: 04°/178°, σ2: 76°/072° and σ3: 14°/267°)**

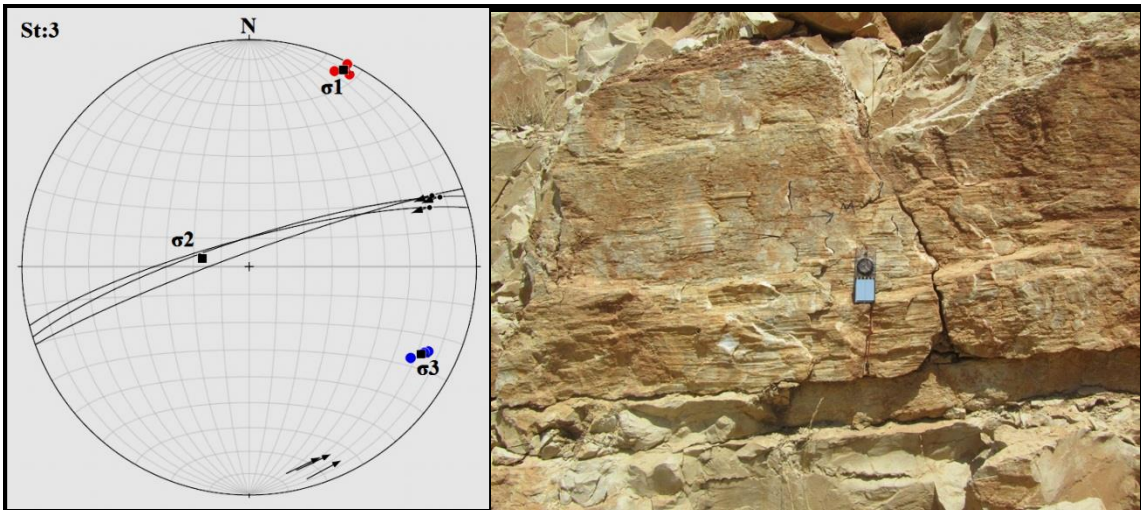

Fig. (28): Fault-slip data analyses with field photo in the station 3 from NW dipping sinistral strike slip faults **.**
(σ1**: 05°/026°, σ2: 73°/281° and σ3: 17°/117°)**

Station four:

Two groups of sinistral strike slip faults were analyzed in station four. The first is southwest dipping faults show that the compression paleostress was in the ESE-WNW direction with maximum stress axis **(σ1: 29°/101°)** (Fig.29). The second group is dipping to the SE direction revealed that the compression paleostress was in the direction NW-SE with maximum stress axis direction **(σ1: 18°/329°)** (Fig.30). These two stress directions were recorded from joints and other mesofaults in other stations.

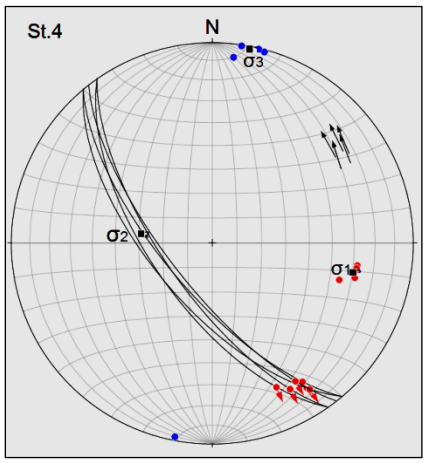

Fig. (29): Fault-slip data analyses with field photo in the station 4 from SW dipping sinistral strike slip faults**.** **(**σ1**: 29°/101°, σ2:61°/278° and σ3: 02°/011°)**

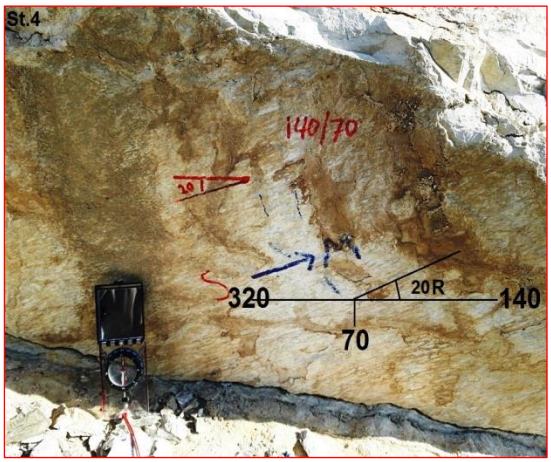

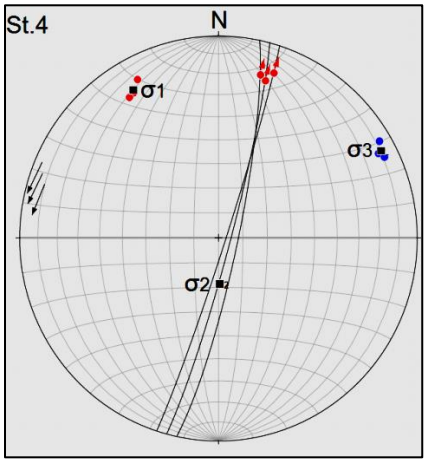

Fig. (30): Fault-slip data analyses with field photo in the station 4 from SE dipping sinistral strike slip faults**. (σ1: 18°/329°, σ2: 69°/182° and σ3: 10°/063°)**

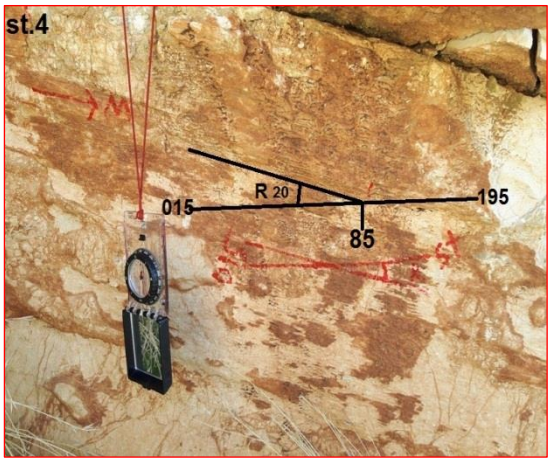

At station (4), a strike slip mesofaults bears two superimposed striation sets. Dextral and sinistral sense of movements (Fig.31 left and right) and (Fig.32). Kinematic analysis of faults slip data revealed two successive stress directions. First (NE-SW) compressive stress which is considerate relatively older than the second (NW-SE). (NE-SW) primary compressive stress which is perpendicular to sub perpendicular to the fold axes seams as a responsible to the initial folding in the area, while the (NW-SE) compressive stress considered as secondary stress state developed in relaxation episode succeeding the primary compressive pulse.

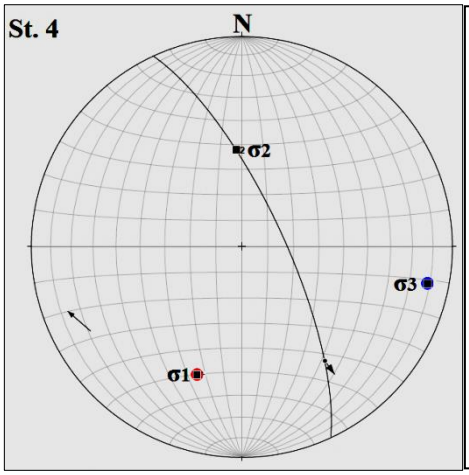

Fig. (31)
Left : NE-SW compressive stress with dextral movement sense.
σ1: 36°/199°
σ2: 52°/357°
σ3: 11°/101°
Right: NW-SE compressive stress with sinistral movement sense.
σ1: 20°/289°
σ2: 70°/100°
σ3: 03°/198°

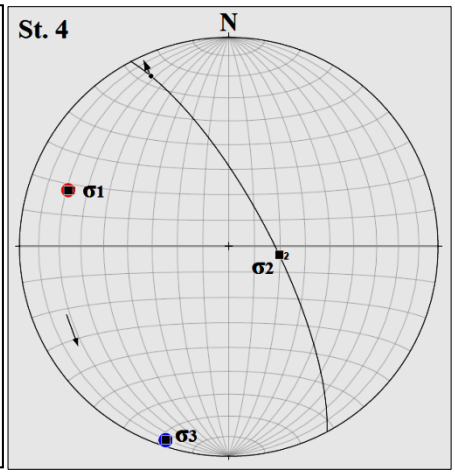

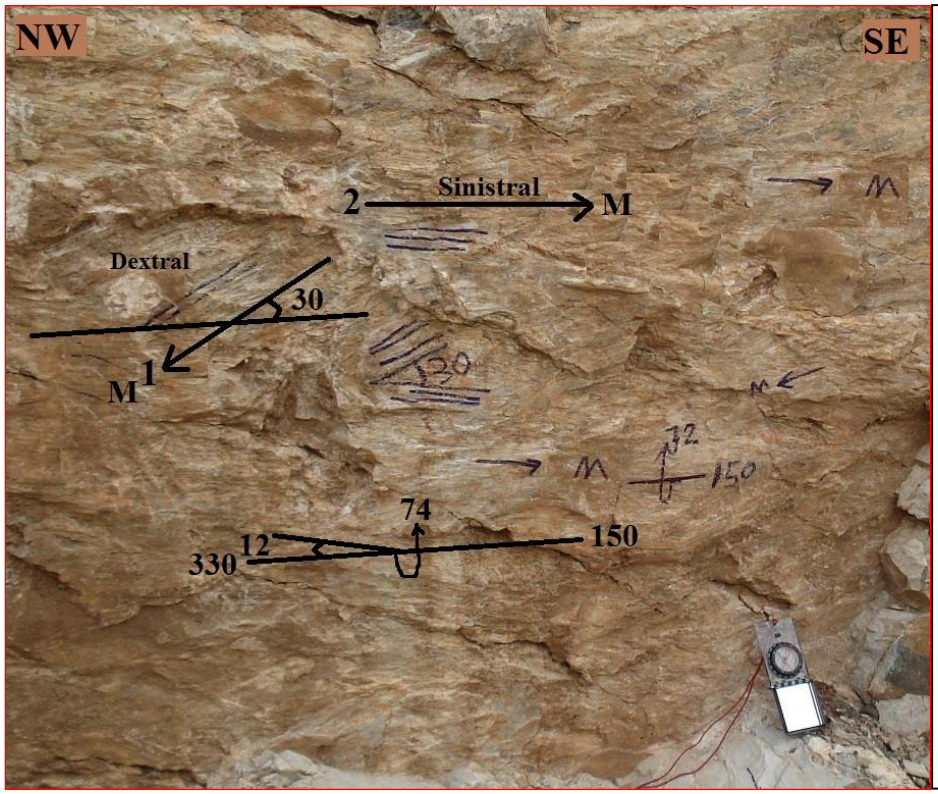

Fig. (32): Two superimposed striation sets on strike slip fault in station 4. The older pitching 30° with fault strike while the younger pitching 12°.

Station five:

Three groups of mesofaults were analyzed in station five. The first is southwestern dipping dextral strike slip faults**.** The compression paleostress revealed from these faults was approximately in the north-south direction with maximum stress axis **(σ1: 19°/001°)** (Fig.33). The second group are three sinistral strike slip faults dipping to the NW direction revealed that the compression paleostress was in the direction NW-SE with maximum stress axis direction **(σ1: 21°/313°)** (Fig.34). Third group are two normal faults dipping approximately to the east revealed that the extension paleostress was in the direction NW-SE with least principal stress axis **(σ3: 27°/111°)** for extensional stress (Fig.35). As we mentioned before (NW-SE) extension face is the byproduct from paleostress in the direction (NE-SW).

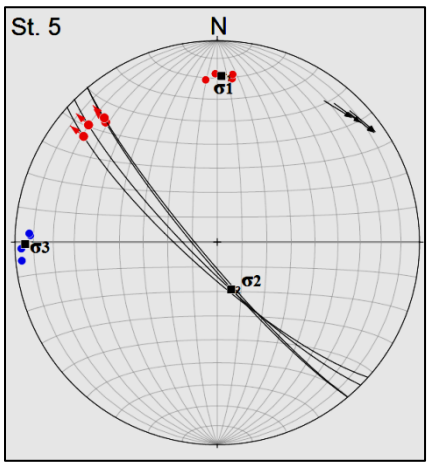

Fig. (33): Fault-slip data analyses for 4 dextral strike slip faults with field photo in the station 5**.** The paleostress are:

(σ1: 19°/001°, σ2: 70°/164° and σ3: 06°/269°)

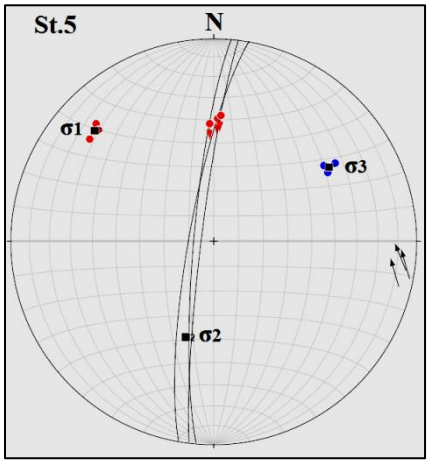

Fig. (34): Fault-slip data analyses for sinistral strike slip faults with field photo in the station 5**.** The paleostress are: **(σ1: 21°/313°, σ2: 49°/196° and σ3: 33°/057°)**

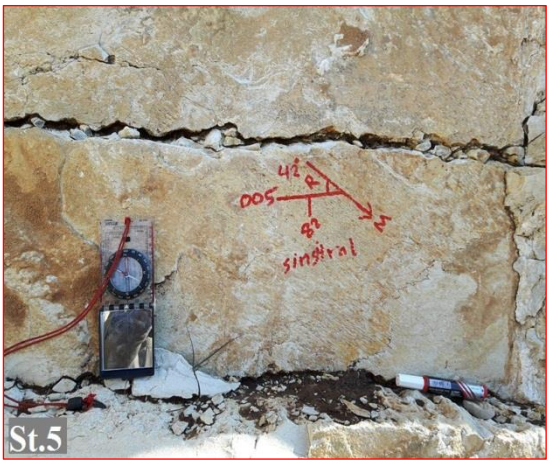

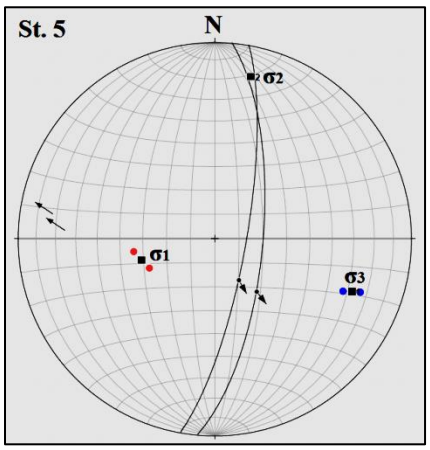

Fig. (35): Fault-slip data analyses for 2 normal faults with field photo in the station 5**.** The paleostress are:

(σ1: 58°/254°, σ2: 17°/013° and σ3: 27°/111°)

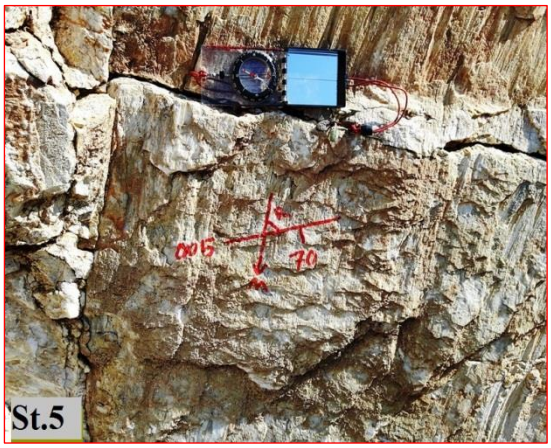

Station six:

In this station three close strike slip faults were analyzed as single faults (Fig.36 and 37). Two are sinistral and one is dextral. The overlapping of three faults show that the stress is rotate clockwise from fault one to fault three, from NE-SW to ENE-WSW. This might be attributed to the oblique collision between the Arabian and Eurasian Plates. *[11]* and *[2]*, and also due to the counterclockwise rotation of the Arabian plate with respect to the Eurasian (Iranian) plates. *[7]*

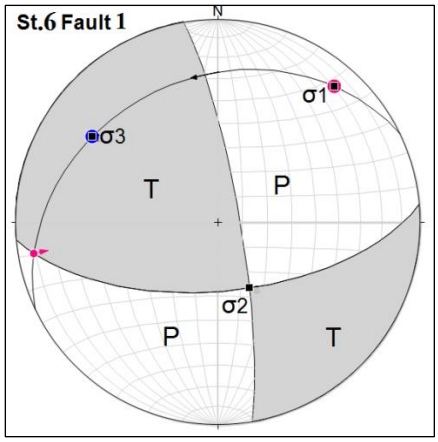

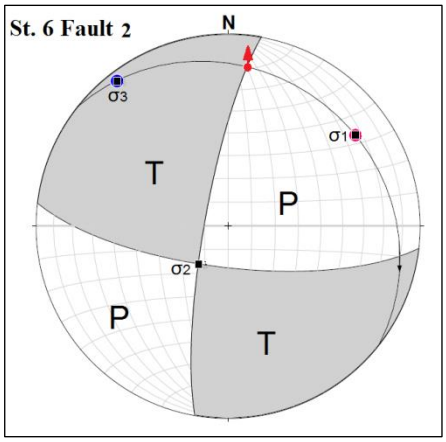

Fig. (36): Stereographic projection of the three faults of the station 6 show Fault-slip data analyses with the overlapping projections of the three faults.

Fault 1: Sinistral: **(σ1: 13°/041°, σ2: 60°/154° and σ3: 26°/304°)**

Fault 2: Dextral **(σ1: 20°/054°, σ2: 70°/218° and σ3: 05°/323°)**

Fault 3: Sinistral **(σ1: 01°/080°, σ2: 45°/171° and σ3: 45°/350°)**

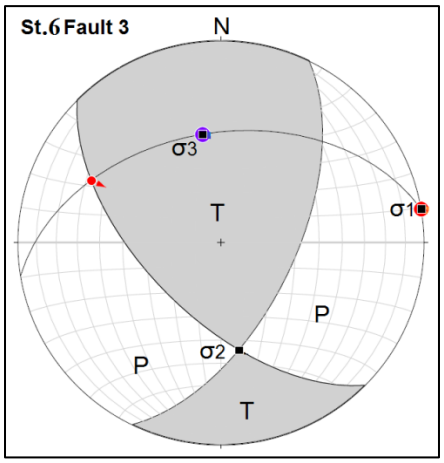

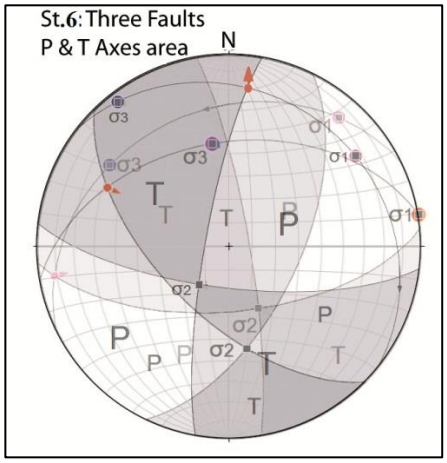

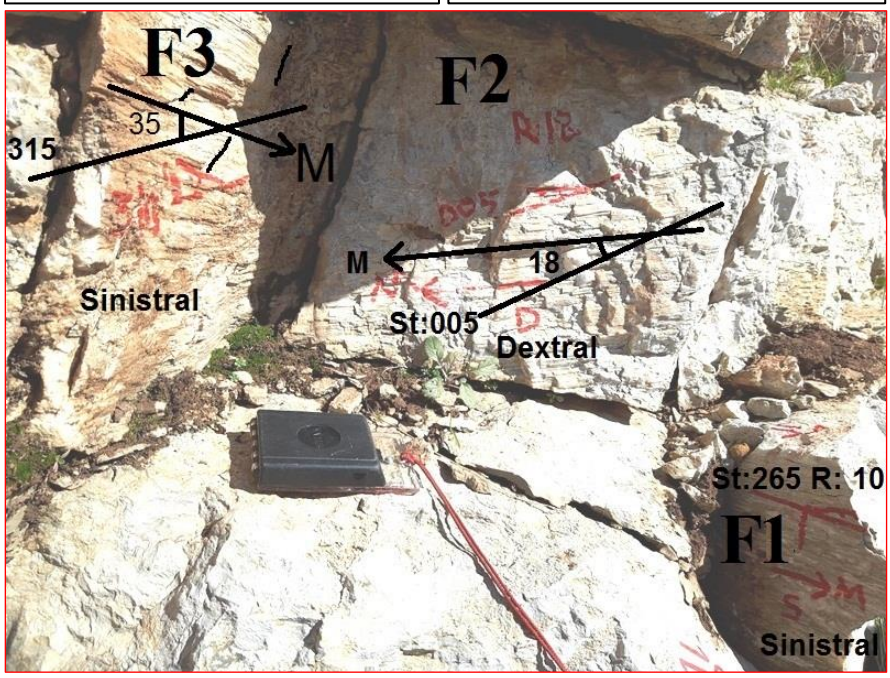

Fig. (37): Prominent striated surface of the three faults (F1, F2, and F3) at station six

The paleostress which obtained from fault slip data summarized in the table two according to the azimuths of their principal stresses. Fifteen paleostress directions were measured distributed in the following directions: **(5** compression paleostresses in the direction **NE-SW) (5** compression paleostresses in the direction **NW-SE) (2** compression paleostresses in the direction **N-S)** (Compression paleostresses in the direction **ENE-WSW)**(Compression paleostresses in the direction **ESE-WNW)** (Extension paleostress in the direction **NW-SE)**

Table (2): Paleostress obtained from fault-slip analysis in the studied area.							
Station No.	Total No. of faults	Type of faults	Maximum stress direction	Principle stress			Stress types
				σ1	σ2	σ3	
1	4	Dextral strike slip	NW-SE	**20°/108°**	**67°/259°**	**10°/014°**	compression
1	5	Sinistral strike slip	NW-SE	**14°/287°**	**76°/101°**	**01°/197°**	compression
2	3	Dextral strike slip	NE-SW	**18°/217°**	**70°/015°**	**07°/125°**	compression
3	4	Sinistral strike slip	N-S	**04°/178°**	**76°/072°**	**14°/267°**	compression
3	3	Sinistral strike slip	NE-SW	**05°/026°**	**73°/281°**	**17°/117°**	compression
4	5	Sinistral strike slip	ESE-WNW	**29°/101°**	**61°/278°**	**02°/011°**	compression
4	3	Sinistral strike slip	NW-SE	**18°/329°**	**69°/182°**	**10°/063°**	compression
4	1	Dextral strike slip	NE-SW	**36°/199°**	**52°/357°**	**11°/101°**	compression
4	1	Sinistral strike slip	NW-SE	**20°/289°**	**70°/100°**	**03°/198°**	compression
5	4	Dextral strike slip	N-S	**19°/001°**	**70°/164°**	**06°/269°**	compression
5	3	Sinistral strike slip	NW-SE	**21°/313°**	**49°/196°**	**33°/057°**	compression
5	2	Normal	NW-SE	**58°/254°**	**17°/013°**	**27°/111°**	extension
6	1	Sinistral strike slip	NE-SW	**13°/041°**	**60°/154°**	**26°/304**	compression
6	1	Dextral strike slip	NE-SW	**20°/054°**	**70°/218°**	**05°/323°**	compression
6	1	Sinistral strike slip	ENE-WSW	**01°/080°**	**45°/171°**	**45°/350°**	compression

2.3: Veins and vein arrays (Tension gashes):

(Bles and Feuga, 1986) *[5]* described veins as tension gashes. They might be associated with stylolite seams indicating the maximum principal stress direction, which is parallel to the long axes of such veins. The morphology of tension gashes shows that they formed under tensile stress.

Station one:

Individual and vein array were recognized in the station one on the joint faces and surface of the bedding planes (Figs. 38& 39). In the figure (38), the gash is in the (bc) joint face, its long axis is parallel to the peaks of the parallel bedding stylolites perpendicular to sub-perpendicular to the bedding planes which is the direction of the maximum stress axis **σ1.**

In sinistral vein array (Brittle shear zone) on the surface of the bedding plane (Fig.39), **σ1** in the direction of the long axis of the approximately sigmoidal tension cashes indicate to the NE-SW.

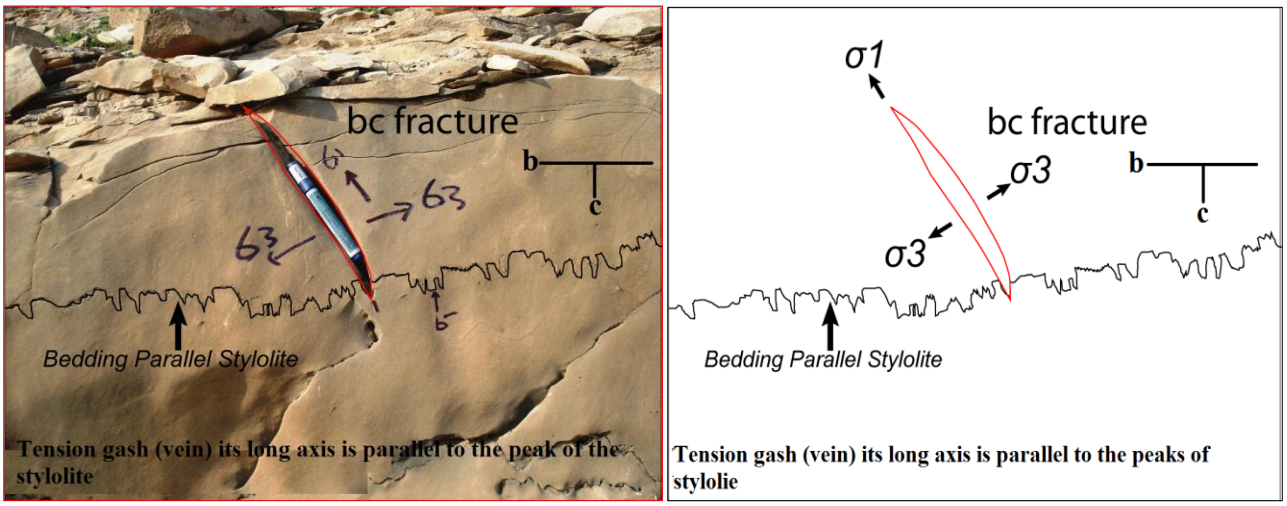

Fig. (38): Tension gash (vein) its long axis is parallel to the peaks of the parallel bedding stylolite.

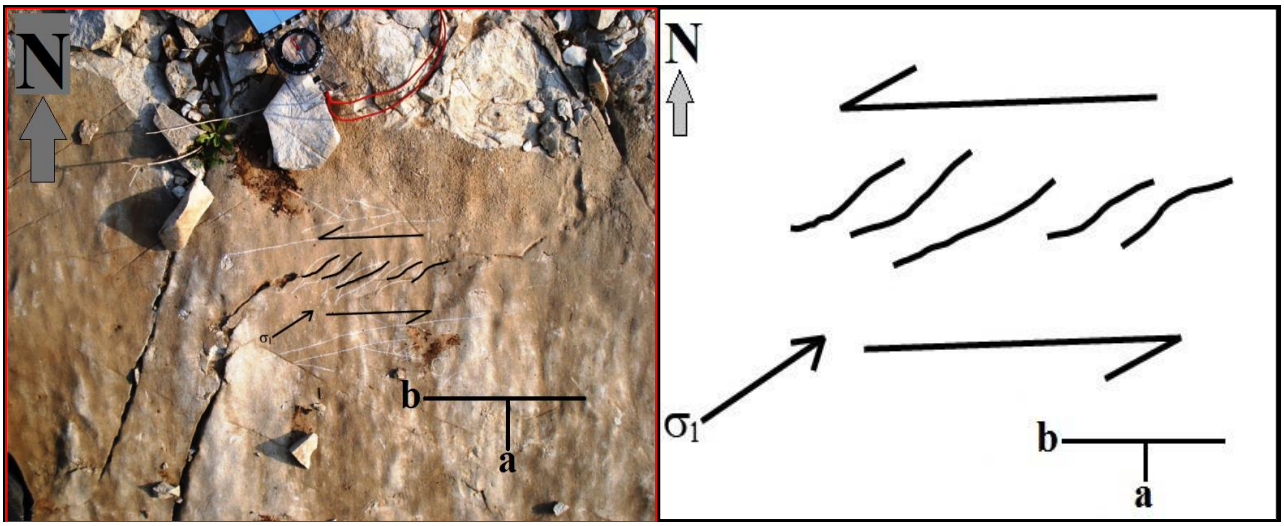

Fig. (39): A sinistral brittle shear zone inclosing enechelon vein arrays on the on the surface of bedding plane in the station one

Station five:

Two stress directions were deduced from sinistral brittle shear zone and two superimposed stylolite seems on the bedding plane (Fig.40).

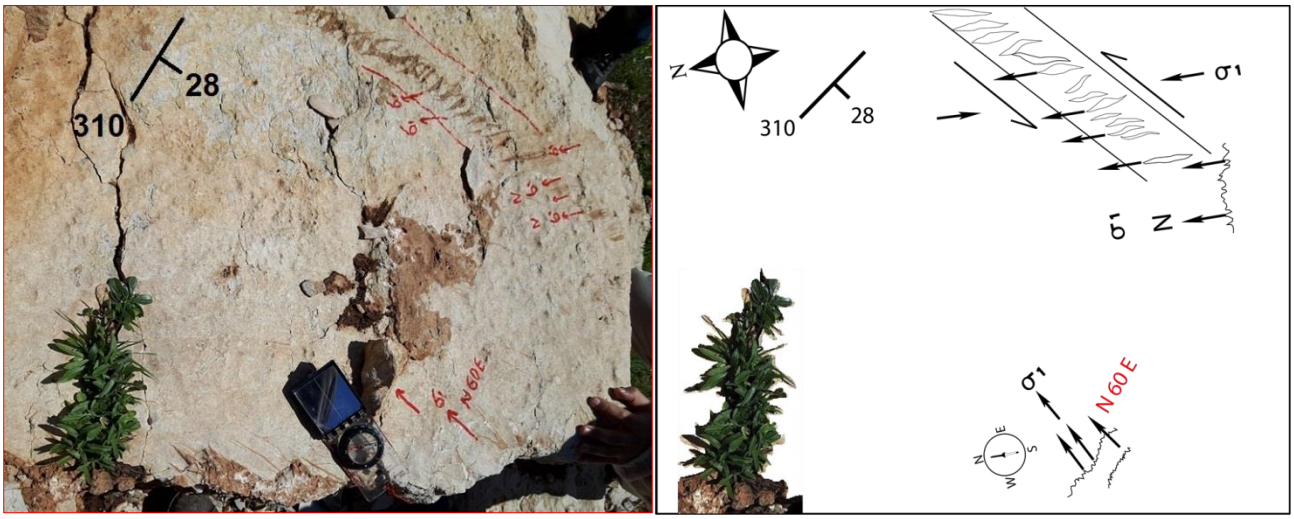

Fig. (40): Sinistral brittle shear zone inclosing enechelon vein arrays on the surface of bedding plane in the station five.

The enechelon vein array and stylolite seems indicate to the relatively earlier N-S compressive stress than the younger N60E primary compressive stress which indicated by stylolite peaks in the southeast corner.

Minor folds in station five:

Two chevrons minor folds (anticline and syncline) were recorded in the southwestern limb of the Kosrat anticline in station five (Fig.41). The folds are Z folds. Pi (π) diagram of the anticline (Fig.42) shows that the fold is asymmetrical with northeast vergence toward the hinge of the major fold. The attitude of the axial plane is **136°/77°**, the average attitude for the northeastern limbs is **145°/53°** and for the southwestern limb is **301°/28°**, and the attitude of the fold axis is **138°/09°**. The interlimb angle is **101 °** and here the fold is open according to (Fleuty, 1964) fold classification. The fold is congruous its axis direction is approximately accordance with the axis of the Kosrat anticline fold axis: **142°/07°.** Hinge space problem of the fold solved by reverse faulting due to lake of incompetent layers. *[9]*

The paleostress direction which is resulted from the pole of the axial plane is in the direction NE-SW with **σ1: 046°/13°).** This stress direction is compatible with primary (NE-SE) paleostress direction in study area. According to the orientation of this minor fold and its relation with the major fold, indicate that it was developed progressively in accordance with major fold development. They might be developed during the tightening stage of the major fold in response to tangential stress directed NE-SW and continued their modification contemporaneously with the major fold.

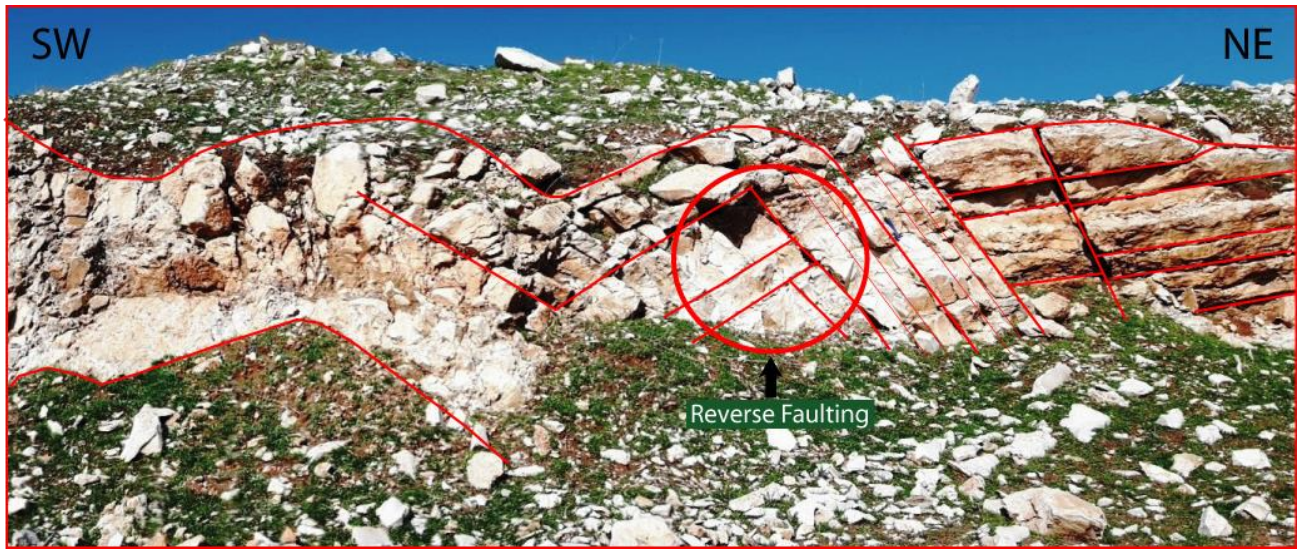

Fig. (41): Chevron minor folds in the station five in southwestern limb of Kosrat anticline.

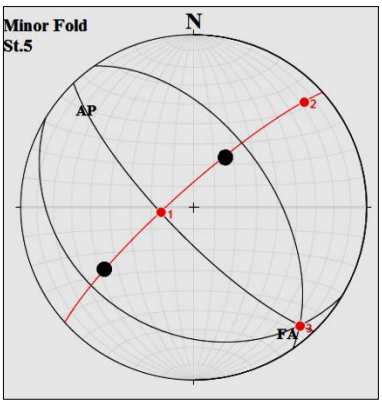

The measurements are in (RHRL)

- NE limb: **145°/53°**
- SW limb: **301°/28°**
- Fold axis: **138°/09°**
- Axial plane: **136°/77°**
- Interlimb angle: **101 °**
- Fleuty classification: **Open fold.**
- Fleuty 1964 classification: **Plunging inclined fold.**
- Congruous minor fold
- 2 is the pole of axial plane

Fig. (42): Stereographic projection of the minor folds in station five showing pi-diagram and fold parameters

2.4: Stylolite seams (Pressure-Solution surfaces):

Kometan Formation is one of the best calcareous environments for stylolite development. They form in preexisting fractured or intact rocks. When the rock compressed from opposite sides they interpenetrate each other due to dissolution of the rock matrix. Very irregular pitted surfaces resulted with alternating peaks and hollows that correspond to each other on the two surfaces (Fig. 43). The peaks oriented parallel to the maximum principle stress orientation. [5] and [16].

Many terms used for describing parallel bedding stylolites and oblique to bedding plane. (Symmetrical and asymmetrical, cylindrical and conical, (Bles and Feuga, 1986), stylolites and slickolites were used for bedding parallel stylolite and oblique stylolite respectively (Ramsey and Huber, 1983 and Haakon Fossen, 2010 *[9]*). The first is thought to be of depositional (digenetic) origin, whereas the latter is of tectonic origin. *[5]*.

Fig.(43): Shows the irregularity of stylolitic bedding plane (compression pitted facets) in Kometan Formation in Dokan area.

Cylindrical and conical stylolites were registered in the limestone beds of Kometan Fn. usually the stylolites associated with the veins (Fig 44). This association interpreted that the dissolution materials from stylolites precipitated in the open veins. Thus shortening of the rock body in a direction is complemented by its stretching at a nearly perpendicular direction. *[13]*. The vertical peaks of the bedding parallel stylolite seams (Fig. 43and 45) tectonically indicate to stretching state with horizontal minimum stress axis σ3.

Figure (44 left) in station (2) shows two sub-orthogonal stylolite seams cylindrical and conical on the **ac** joint face. The peaks of conical pointed approximately along dip direction of the bedding planes and it is compatible with the main compressive stress **σ1** in the direction NE-SW.

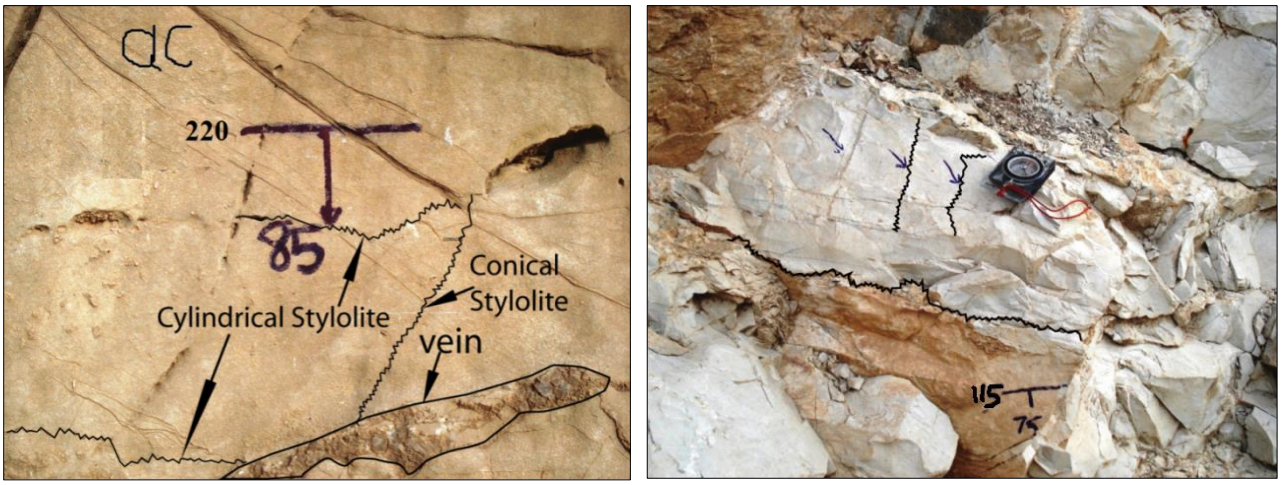

Fig.(44): Left; cylindrical and conical stylolites on the (ac joint face) in the station (2). Right; cylindrical and conical stylolites on the (bc joint face) in the station (3).

(Fig. 44 right) in station (3) shows cylindrical and three conical stylolite seams on the fracture face with strike approximately parallel to the strike of the bedding planes it is seems to **bc** joints. There for the conical stylolites pointed approximately along strike direction which is indicate to the maximum compressive stress **σ1** in the direction NW-SE**.** Figure (45) station (4) shows the two types of stylolite cylindrical and conical on the **bc** joint face. The peaks of the conical stylolite seems indicate to maximum compressive stress **σ1** in the direction NW-SE.

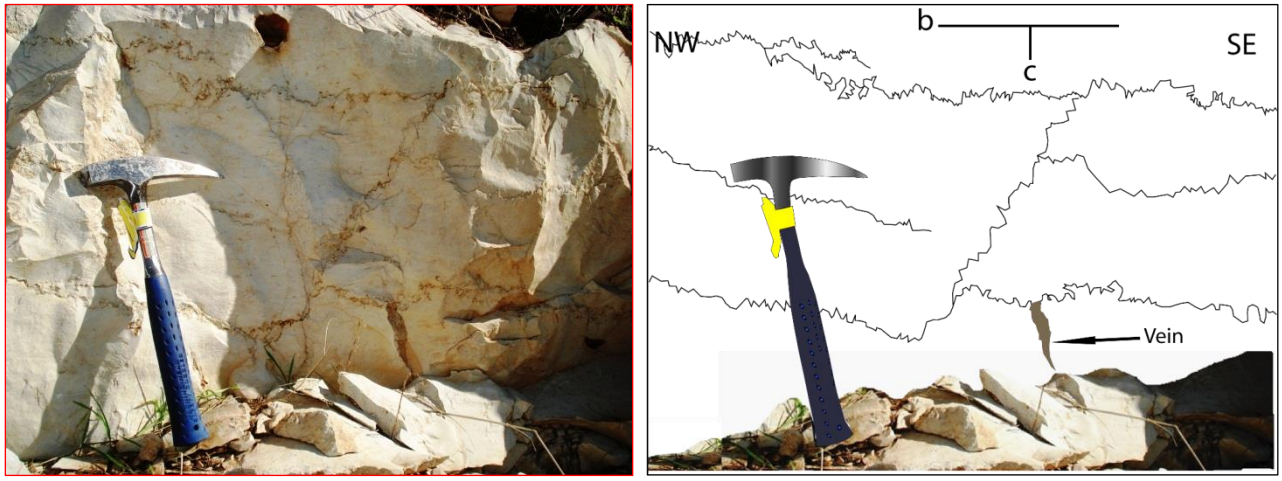

Fig.(45) stylolites in station 4 cylindrical and conical stylolites on bc joints

3: Discussion:

Joints, mesofaults, veins, stylolite seams were studied through (7) stations in Kosrat anticline. Two orthogonal joint tension sets ac and bc together with following shear systems [(hkO) acute about (a), (hkO) acute about (b) Okl acute about (b), Okl acute about (c) and hOl acute about (c)] where distinguished in the study area. It is clear from table one listed above that the most prevalent paleostress directions are (NE-SW and NW-SE). The first (NE-SW) compressive stress normal to the general trend of the major anticline considerate as horizontal primary component of oblique collision between Arabian Plate and Eurasian. This compressive phase led to initiation (ac) tension set and (hkO) acute about (a). (bc) tension set, (hkO) acute about (b) and (Okl) acute about (b) indicate that they formed by other compressive stress in the direction NW-SE parallel to sub parallel to the axes of the major fold. This stress considered as secondary stress developed during relaxation event after primary compressive stress. (hkO) acute about (b) tectonic axis is one of the most prevalent shear fractures in the study area. Open fissures occurred along (hkO) acute about (b) in the azimuth direction (330°). These open fissures may be is one of the causes of rocks fall in the road between Dokan and Ranyah.

The approximately vertical (σ1) which analyzed from (hOl) acute about (c) and (Okl) acute about (c) shear joints indicate that these joints may be developed by the extensional phase associated with NE-SW and NW-SE compressive stresses.

The multi trends of paleostress in the directions (NE-SW) perpendicular to sub-perpendicular to the general trend of the anticline with following direction maximum stress **(σ1) (29/226), (07/022), (13/219), (21/207) and (38/208)** might be attributed to the oblique collision of the Arabian and Eurasian plates along their zigzag margins.

Other subordinate paleostress is in the direction (NW-SE) with maximum stress directions of **(σ1) (03/308), (07/307), (07/119), (02/299) and 04/309.** This stress can be considerate as secondary stress developed during the relaxation of the succeeding primary stress with **(σ3)** in the direction (NE-SW)

Different orientations of striated mesofaults assemblages were measured in the study area, which has different orientations with respect to the axis of their enclosing fold (table two above). The most dominated types are strike slip displacements faults. Both dextral and sinistral follow or occupy either (hkO) acute about (a) or (b)

joint systems as preexisting fractures for these faults. From these striated mesofaults the following paleostress directions were detected:

Compressive stress in the directions (N-S), (NE-SW), (ENE-WSW), (WNW- ESW), (NW-SE) and extension stress in the direction (NW-SE). All these paleostress directions revealed also from joints, except N-S directions. However the NE-SW and NW-SE paleostress directions are most prevalent than other directions. (NE-SW) seams as a responsible to the initial folding with maximum stress directions **(σ1) (18°/217°), (05°/026°), (36°/199°), (13°/041°), (20°/054°) (Fig.)**

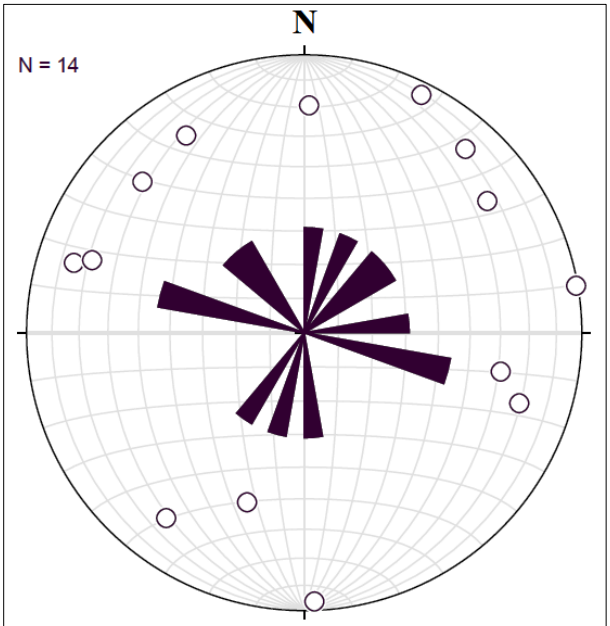

Palestress stress directions from striated faults in the study area

The over lapping of three close faults in station six show the clockwise rotation of stress from NE-SW to ENE-WSW This might be attributed to the oblique collision between the Arabian and Eurasian Plates. [11] and [2], and also due to the counterclockwise rotation of the Arabian plate with respect to the Eurasian (Iranian) plates. [7]

The two superimposed striation sets in the station 4 revealed two successive stress directions (NE-SW) compressive stress considerate relatively older than (NW-SE). (NE-SW) primary compressive stress which is perpendicular to sub perpendicular to the fold axes seams as a responsible to the initial folding in the area, while the (NW-SE) compressive stress considered as secondary stress state developed in relaxation episode succeeding the primary compressive pulse.

Furthermore, some of above paleostress directions were verified also by analysis of other kinematic indicators in the study area these are; pressure solution surfaces (stylolite seams), planner veins (Tension gashes), and brittle shear zones. The stylolites and veins are existing in the same outcrop close to each other.

Conical and cylindrical stylolites recognized in the study area. The first is of tectonic origin, whereas the later thought to be of depositional (digenetic) origin. The vertical peaks of stylolite seems in the (Figures 38, 43and 46) in bedding parallel stylolite and individual veins indicate to stretching state with horizontal minimum stress axis (σ3) normal to the major fold trend resulted from final uplifting of folds. While the peaks of the conical stylolite seams on joint faces indicate to the two sub orthogonal compressive stress regimes (NE-SW and NW-SE) (figures 44 and 45). The stylolite peaks in the figure 40 indicate to the (N-S) and (NE-SW) directions.

In sinistral vein array (Brittle shear zone) on the surface of the bedding plane (Fig.39), σ1 in the direction of the long axis of these tension cashes indicate to the (NE-SW) compression paleostress direction while in the sinistral brittle shear zone in the station five (Fig.40) the long axis of the gashes indicate to the (N-S).
Moreover, it is quite clear that the primary paleostress (NE-SW) cause in the development of congruous minor fold in the SW limb of Kosrat anticline (Fig. 41 station five)
First compressive tectonic phase in the direction (NE-SW), this was responsible for initial folding and forming the brittle failure structure stage. Second compressive tectonic phase was active in the direction (NW-SE) which caused change in direction of axes of folds generated from first tectonic phase and generation of new brittle failure structures and developed the first brittle failure structures.
The authors who have investigated paleostress in study and surrounded areas are as following:
Al Fadhli et al., (1979 and 1980) *[17]* and *[18]* studied poly-phase deformation and superimposed folding in Piramagroon, Surdash and Sayed-Sadek folds. They have pointed to three compressive tectonic phases that detected also in this work. First and second phases were coaxial and in the direction NE-SW and they responsible for early folding of the major folds. Third phase was in the direction (NW-SE) approximately normal to the first two. The compression tectonic stresses in the directions N-S and (ENE-WSW) with extension phases which were detected in this work are not mentioned.
Taha et al., (1995*) [19]* studied Microtectonic in the Dokan area and distinguished only three tectonic phases from veins and stylolite seams: Two compressive tectonic phases (NNE-SSW and EW) directions and third was extension phase in the direction 160^0. The first and third phases were detected also in present study while the second phase is not compatible with stresses which detected in this study. Other tectonic stresses (compression and extension phases in the NW-SE) are not mentioned in by these authors.
Al-Jumaily (2004) *[1]* Studied tectonic investigation of the brittle failure structures in the foreland fold belt in northern Iraq and he deduced two compressive tectonic stresses:
First compressive tectonic phase in the direction (N-S and NE-SW) and (E-W and SE-NW). These tectonic regimes somewhat are compatible with that which detected in present study, and he attributed the reorientation of the stress field from one direction to another to the oblique collision between the Arabian and Eurasian plates and to the anticlockwise rotation of the Arabian plate relative to Eurasian plate.

4: Conclusions: The main conclusions of present work can be summarized as follows

1) New geological map and cross section were drawn in the study area.
2) Paleostress analysis from minor structures (joints, mesofaults, veins and stylolite seams) indicated that the investigated area was subjected throughout its geological history to four stress states. Two of them are compression and two are extension.
3) The primary stress is the compressive stress with their maximum horizontal axis (σ1) in direction (N-S), (NE-SW) and successive phase in the direction (ENE-WSW) which are seam as a responsible to the initial folding and most of brittle failures in the area.
4) The (NW-SE) compressive stress parallel to sub parallel to the fold axes considered as secondary stress developed during relaxation event succeeding the primary compressive pulse. This stress is responsible to the other brittle failures in the area.
5) The (NE-SW) extension stress considered as a releasing phase that associated with the final uplift of the main fold.
6) NW-SE extension face considerate as extension stress related to the primary NE-SW compressive stress.
7) The paleostress phases which detected from joints and fault slip data analysis were verified from veins and stylolite seams analysis.

5: References:

[1] AL-Jumaily, I.S.I. "*Tectonic investigation of the brittle failure structures in the Foreland Folds Belt"*. Northern Iraq, Unpub. Ph.D thesis, University of Mosul, Iraq, (in Arabic).(2004).

[2] Aswad, K.J. " *Arc-Continent Collision in Northeastern Iraq as evidence by the Mawat and Penjwin Ophiolite Complexes".* Raf. Jour. Sci., 10(1), pp. 51-61. (1999).

[3] Anderson, E, M. "*The dynamics of faulting. 1st ed*.", Oliver and Boyed, Edin- burgh, 206p.(1942).

[4] Angelier, J. and Mechler, P. "*Sur une methode graphique, de recbercbe des contraintes enseismologie: La methode de diedres droits"*. Bull. Soc. Geol. France, 7, pp.1309-1318.(1977).

[5] Bles, J. L. and Feuga, B. *"The fracture of rocks. North Oxford Academic publishers Ltd."*, 131p. (1986).

[6] Hancock, P.L. *"Brittle microtectonics: principles and practices".* J. Struct.Geol., 7, pp. 437-457. (1985).

[7] Hancock, P.L. and Atiya, M.S. *"Tectonic significance of mesofracture systems associated with the Lebanese segment of the Dead Sea fault*". J. Struct. Geol., 1, pp.143-153.(1979).

[8] Hancock, P.L. and Alkadhi, A. and Sha'at, N.A. *"Regional joint sets in the Arabian platform as imdicators of intraplate processes"*. Tectonics, Vol3, pp.27-43.(1984).

[9] Haakon Fossen. "Structural geology" Cambridge University Press, New York, USA, 463p. (2010)

[10] Lisle, R.J. *"Principal stress orientation from faults: An additional constraint".* Ann. Tectonics, 1, pp.155-158.(1987).

[11] Numan, N. M. S. *" Discussion on "Dextral Transpression in Late Cretaceous Continental Collision, Sanandaj - Sinjar Zone, Western Iran*". J. Struct. Geol Vol. 23. (2001b)

[12] Ramsay, J. G and Huber, M. I. *"The techniques of modern structural geology"* V.2, Folds and Fractures. Academic press, London, 700p. (1987).

[13] Suppe, J., 1985**.** *"Principles of Structural Geology"* Prentice-Hall, Inc, New Jersey, 537p.

[14] Turner, F.J. and Weiss, L.E. *"Structural analysis of metamorphic tectonite"* McGraw-Hill, New York, 545p.Vol3, pp.27-43. (1963).

[15] Twiss, R. J. and Moores, E. M. *"Structural geology"* W.H. Freeman, USA, 717p.(2007).

[16] Van der Pluijm, B.A. and Marshak, S. *"Earth structure: An introduction to structural geology and tectonics"*. WCB/McGraw Hill, USA, 495p. (2004).

[17] AL-Fadhli, I., Janardan Rao, Y., Oweiss, G. and Khalil, M. "*Polyphase deformation in apart of Zagros. Sulaimaniyah district, NE Iraq"*. J. Indian Academy of Geoscience. 22, pp.1-31.(1979).

[18] AL-Fadhli, I., Janardan Rao, Y., Oweiss, G. and Takla, M.A. "*Superimposed Folding in Sayed-Sadek area, near the Zagros suture zone",* Iraq. Geoviews, VIII, No.111, pp.126-148.(1980).

[19] Taha, M.A., Al-Saadi, S.N. and Ibrahim, I.S. *"Microtectonic study Dokan area NE Iraq"* Iraqi Geol. Soc. Jour., 28 (1), pp.25-35.(1995).